Yarmouk University
Hijjawi Faculty for Engineering Technology
Department of Computer Engineering

Unity Power Factor Speed Sensorless Control of Permanent Magnet Synchronous Motors

M.Sc. Thesis

By

Hakam Suleiman Shehadeh

Advisor

Dr. Mohammad Al-Zoubi

Co-Advisor

Dr. Sami Al-Hamdan

August, 2011

Unity Power Factor Speed Sensorless Control of

Permanent Magnet Synchronous Motors

By
Hakam Suleiman Nu'man Shehadeh

B.Sc of Industrial Automation Engineering, Electrical Engineering
Department, Palestine Polytechnic University, Palestine 2007

A thesis Submitted In partial fulfillment of the requirements for the

degree of Master of Science, in the Department of Computer

Engineering, Yarmouk University, Irbid, Jordan

Approved by:

Dr. Mohammad Al-Zoubi ....Chairman
Associate Professor of Electrical Power Engineering, Yarmouk University

Dr. Sami Al-Hamdan...Member
Associate Professor of Computer Engineering, Yarmouk University

Dr. Ibrahim Al-Tawil...Member
Associate Professor of Electrical Power Engineering, Yarmouk University

Dr. Amin Alqudah..Member
Assistant Professor of Computer Engineering, Yarmouk University

II

Dedicated to my parents, my wife and my son: OMAR

١

ACKNOWLEDGMENTS

I would like to thank my adviser Dr. Mohammad Al-Zoubi and co-advisor Dr. Sami Al-Hamdan for their assistance, direction and guidance. I also wish to express my deep gratitude to all my family members, my parents and my wife, for their support and love; specially my beloved wife Amal for her understanding and sacrifices during my study. Special thank to the DAAD for offering me this valuable scholarship.

TABLE OF CONTENTS

LIST OF FIGUIRS

LIST OF TABLES

١

LIST OF ABBREVIATIONS

ABBREVIATIONS	Name
AC	Alternating Current
DC	Direct Current
PMSM	Permanent Magnet Synchronous Motor
IPMS	Interior Permanent Magnet Synchronous Motor
SPMS	Surface-mounted Permanent Magnet Synchronous Motor
FOC	Field Oriented Control
DTC	Direct Torque Control
PI	Proportional - Integral
UPFC	Unity Power Factor Control
UPF	Unity Power Factor
PF	Power Factor
MTPAC	Maximum Torque Per Ampere Control
CTAC	Constant Torque Angle Control
CSFC	Constant Stator Flux Control
MMF	Magnomotive Force
VSI	Voltage Source Inverter
PWM	Pulse Width Modulation
FWC	Field Weakening Control
MRAS	Model Reference Adaptive System
SMC	Sliding Mode Control
FLC	Fuzzy Logic Controller

LIST OF SYMBOLS

Symbol	Name
v_d	the d-axis stator voltage (V)
v_q	the q-axis stator voltage (V)
R_s	Stator resistance (Ω)
i_d	the d-axis stator current (A)
i_q	the q-axis stator current (A)
ω_e	the rotor's electrical angular velocity (rad/sec)
ω_m	the rotor's mechanical angular velocity (rad/sec)
λ_d	the Stator Flux Linkages in d-axis (H)
λ_q	the Stator Flux Linkages in q-axis (Wb)
λ_m	The Flux Linkage of the PM (Wb)
L_d	the d-axis stator inductance (H)
L_q	the q-axis stator inductance (H)
Te	The developed torque (N.m)
T_L	The load torque (N.m)
B	The viscous friction coefficient (N.m.s)
J	The moment of inertia (kg.m^2)
P	Number of poles
θ_r	The rotor position angle
f	the frequency (Hz)
P	Active power (W)

S		Apparent Power (VA)
Q		Reactive Power (VAR)
Φ		The phase angle between the voltage and current
v_s		Stator voltage vector (V)
i_s		Stator current vector (A)

ABSTRACT

There are several control approaches of Permanent Magnet Synchronous Motors drive systems. In this work, a new unity power factor controller of three-phase surface-mounted permanent magnet synchronous motor with Fuzzy Logic based Model Reference Adaptive System for sensorless speed control has been developed. The presented work ensures a unity power factor operation of the motor such that the motor's current and voltage are in phase. Speed control of the motor has been achieved using a Model Reference Adaptive System which estimates the motor speed without using a mechanical speed sensor. A fuzzy logic control in conjunction with the Model Reference Adaptive System was used to decrease the steady state error between the actual and the estimated motor speed under different loads and speed commands.

The controller is modeled and simulated using Matlab/Simulink simulation software. A comparison between the Maximum Torque Per Ampere Control and Unity Power Factor Control has been made. Another comparison between the fuzzy logic Model Reference Adaptive System and sliding mode MRAS has confirmed the robustness of the modeled speed sensorless control system under different load and speed commands. Many simulation results and study cases has been conducted and confirmed the validity and the accuracy of this control approach.

Keywords: Permanent Magnet Synchronous Motors, Unity Power Factor Control, Speed Sensorless Control, Model Reference Adaptive System, Sliding Mode Control, Fuzzy Logic Control.

Chapter 1 INTRODUCTION

1.1 Background

Permanent Magnets Synchronous Motors (PMSMs) have been widely used in a variety of applications that require high performance such as fast acceleration and dynamic response, high power density, high efficiency and full torque control [1, 2, 5-27]. DC motors have good dynamic response compared with AC motors, such that the flux and speed can be controlled independently. However, it is difficult to do the same with AC machines using conventional V/f control. The difficulty is attributed to the existence of the coupling between the stator and the rotor in AC machines. This coupling is described by using complex differential equations with time varying rotor position dependant mutual inductances between the stator and rotor. The application of vector control improves such performance and leads to a dynamic performance similar to that of the separately excited DC motor. Furthermore; the huge developments in Power Electronics and semiconductor devices in line with different and improved converter techniques made the AC machines and its drive systems play the main role in the variable speed motor control systems.

In general, PMSM`s are composed of the stator and the rotor. The stator part is the external or outer fixed part where a three phase AC windings are distributed inside the slots to produce the rotating magnetic field. The rotor part which rotates synchronously with the frequency of the stator windings consists of Permanent Magnets (PM) to produce the

magnetic field. This structure produces a sinusoidal back electromotive force (back-EMF), and it can be categorized into two types: 1) Surface-mounted Permanent Magnets Synchronous Motors (SPMSM) and 2) Interior Permanent Magnets Synchronous Motors (IPMSM). In the first type; the permanent magnets are mounted on the surface of the rotor. This structure eliminates the saliency effect since the permeability of the permanent magnets is very close to the permeability of the air. Therefore, the quadrature-axis inductance of SPMSM is equal to the direct-axis inductance, i.e. $L_q=L_d$. On the other hand, in the second type of PMSM, the permanent magnets are buried inside the rotor and the air gap is physically a uniform air gap. However, the equivalent air gap will not be uniform and the saliency effect will appear i.e. ($L_q>L_d$). These different types of PMSM will make the control algorithm different for both types and the produced torque will be dissimilar, too. It is convenient to mention that the mathematical model of SPMSM is simple compared with that of IPMSM. This is because the SPMSM has no saliency, i.e. the motor has equal inductance in direct and quadrature axis.

Several research works were conducted with different control approaches of PMSMs drive systems. Based on the control application, V/f control, Field Oriented Control (FOC) or Direct Torque Control (DTC) can be used. Moreover, many different strategies can be implemented by controlling the stator currents. These different strategies are Unity Power Factor Control (UPFC), Maximum Torque Per Ampere Control (MTPAC), and Constant Stator Flux Control (CSFC) [8].

Among different strategies mentioned above, UPFC is chosen. The key point in UPFC is to operate the motor by keeping the power factor value equals to one; i.e. the motor's currents and voltages will be in phase. This control technique has the advantage of

extending the constant torque region i.e. the motor can operate above its base speed and produce its rated torque. Moreover; the inverter will be fully utilized by supplying real power to the motor and getting higher output power from the motor. This control technique can be done by calculating the reference direct axis current i_d or controlling the phase angle of the stator current.

The rotor position information is important in order to implement and achieve the different control algorithm mentioned above; this can be done by using a mechanical encoder to measure the rotor speed and position. On the other hand, the existence of the mechanical sensor reduces the robustness and reliability of the controller, and increases the overall cost of the drive system. Many research efforts have been made in order to estimate the rotor speed and position without using mechanical sensors; these systems are then known as Sensorless speed Controllers. Fuzzy Logic Controller (FLC) can be used instead of the regular speed PI controller as a speed controller. Some applications need the condition of operating the motor above its base speed and keeping the produced torque at its maximum values. This can be achieved by operating the motor under unity power factor control and as mentioned above extending the constant torque envelop but only for a small range of speed. The field weakening technique then can be applied (if necessarily) if the required speed is very high making it difficult to be achieved using UPFC.

1.2 Literature Review

The technique of UPFC is controlling the motor's currents and voltages such that they will be always in phase. This will fully utilize the inverter and yield an extended constant torque region. The motor can operate above its base speed and produce its rated torque. The authors in [5] applied the UPFC by using two different techniques, the first one controls the direct axis current I_d, while the second controls the angle of the command stator current as in [6]. Also the advantages and drawbacks of the UPFC were demonstrated. In [7], a UPFC was introduced that works with the field weakening (FW) technique by controlling the stator flux linkage. Also, a speed sensorless drive system was achieved. In [8], the author analyzed different control strategies for PMSM including the UPFC, MTPAC and CSFC.

Many other control strategies of field weakening were developed based on analytical methods and look-up-table methodology [9]. The Look-Up-Table (LUT) technique refers to storing the points of d-q currents for optimum operation. In [10, 11], the authors proposed a field weakening operation and the FW mode was divided into three regions in order to achieve a deep filed weakening. A Single Current Regulator (SCR) and Voltage Angle Control (VAC) were used together in [10] in order to fully utilize the DC bus voltage rather than using a single current regulator. While in [11] a single current regulator was used and a fixed value of the q-axis command voltage control scheme was implemented.

Operating the motor below the rated speed (Constant Torque mode), and for efficiency optimization, the control mode below the motor's rated speed is often chosen to be the MTPAC which have been demonstrated in [12-15]. In [14, 15], a flux control algorithm of

4

١

PMSM was investigated using MTPAC in constant torque mode and Flux-Weakening Control (FWC) in constant power mode.

The position and speed sensor reduction in controlled drive systems is a major demand to increase the robustness and reliability of the drive system and reduce the overall cost [16-28]. Many techniques have been developed and implemented in the field of position and speed estimation of the rotor, the rotor position is required in PMSMs drive system, such that the estimated speed is compared to the reference speed in traditional PI or FLC. Many speed estimation methods based on the measured currents and voltages of the PMSM were developed. This has been done by measuring the stator currents or voltages as in [16], or calculating the stator flux to estimate the rotor position [17], or measuring the back EMF [18].

A model reference adaptive system (MRAS) can be used to estimate the rotor position and speed [19]. A reference model that contains the desired mathematical model and an adaptive model is used to adapt the reference model in the MRAS. The rotor speed is generated from the adaptation mechanism using the error between the estimated quantities obtained by the two models.

Regarding the sensorless technique and among all the different methodologies of estimating the rotor speed and position, the Sliding Mode Observers (SMO) are more advantageous in robustness to disturbances and parameter variations [20-26]. The SMO uses a sign-function of the estimated error as a feedback correction. In [26], a SMO based on feedback of equivalent control was proposed and tested for SPMSM and showed its ability to work over a wide speed range.

FLC has been widely used in many drive systems. It can be used to replace the PI controllers for speed control of motors. FLC can be used also to work with MRAS. In [28-30], a speed sensor used to measure the motor speed and compared with the reference speed, the error signal between them is used as an adaptation mechanism to overcome the problem of motor parameter change. In [31, 32], FLC was used to tune the proportional and integral constants of the PI controller used in MRAS. However, the steady state error between the actual and estimated speed still exists. Regarding the system in [33, 34], the FLC replaced the PI controller used in MRAS to estimate the rotor speed of induction motors and solve the optimization problem.

1.3 Objective of the study

This work aims to design a speed sensorless control of SPMSM and be capable of operating at unity power factor condition. A UPF (Unity Power Factor) controller (under constant torque mode) will drive the motor to fully utilize the inverter and extend the constant torque envelope of the motor.

A new UPFC controller with a Modified Model Reference Adaptive based system incorporated with the concept of FLC for estimating the rotor speed and position angle of SPMSM has been developed and tested. This Speed estimation technique for the SPMSM enhances the accuracy of the estimated speed since the used MRAS technique alone doesn't necessarily ensure the convergence and accuracy of the steady state error.

1.4 Thesis Organization

This thesis is arranged as follows; Chapter one contains the background of the study and the objective of the study. Chapter two discusses the construction and the mathematical modeling of SPMSM. The basic operation of SPSM is also presented. In Chapter three a new unity power factor controller of SPMSM is introduced and review of the power factor and power triangle are studied.

Chapter four discusses the MRAS for speed estimation of SPMSM and the possibility to improve the performance and speed estimation of the drive system. Sliding Mode concept and FLC are presented and discussed to work with the MRAS. Chapter five presents the simulation results of the modeled drive system and proves the validity of the system for both UPFC and MRAS. Finally, Chapter six presents conclusions and future work.

7

Chapter 2 PERMANENT MAGNET SYNCHRONOUS MOTORS, MODELING AND OPERATION

This chapter reviews the mathematical model of PMSM of surface type and presents the general model of the motor which is used in the control algorithm. The operation of PMSMs also has been reviewed and the dynamic simulation model of the SPMSM is modeled based on the general mathematical model equations using Matlab/Simulink software.

2.1 Introduction

PMSM has recently played a major role in different industrial drive systems and applications because of its useful features; such as high efficiency, high torque to inertia ratio, high power factor and fast dynamic response. PMSMs are named "Synchronous" because of the fact that they rotate at the same speed as the rotating magnetic field produced by the stator winding, i.e. its speed is related to the input line frequency [1, 2].

The stator windings of PMSM are energized by a three-phase voltage source to produce the rotating magnetic field that interact with the rotor filed as shown in Figure 2.1. The stator windings are distributed inside the slots and displaced by 120 electrical degrees from each other to produce a sinusoidal Magnomotive Force (MMF).

8
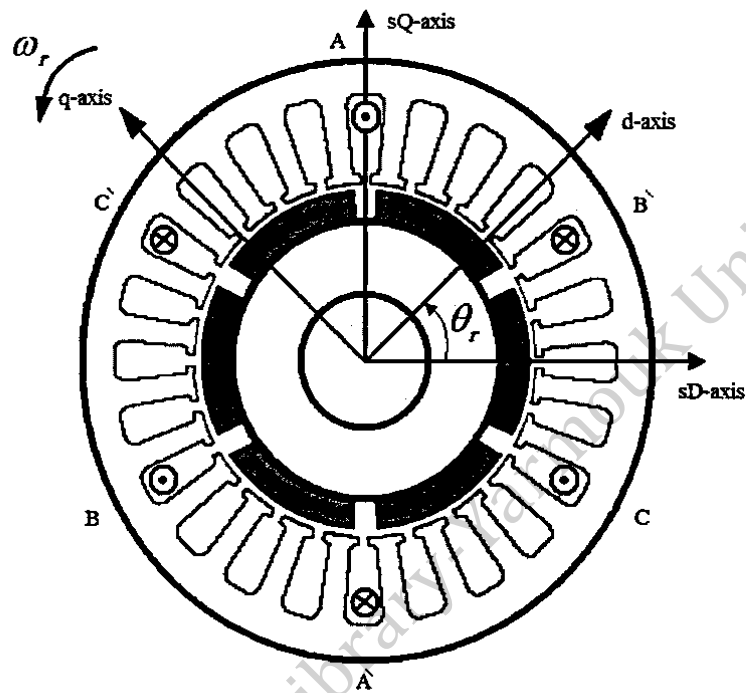
Figure 2.1: Cross-section of a symmetrical three-phase SPMSM with dq axis

On the other hand, the rotor filed is produced by permanent magnets (PM) which is considered as a constant field and cannot be easily controlled as conventional synchronous motors which have a rotor windings fed with a DC power supply. These permanent magnets can be positioned on the rotor in two different ways; in the first configuration, the PMs are mounted on the surface of the rotor as shown in Figure 2.2, this type is then called surface-mounted PMSM or SPMSM.

9
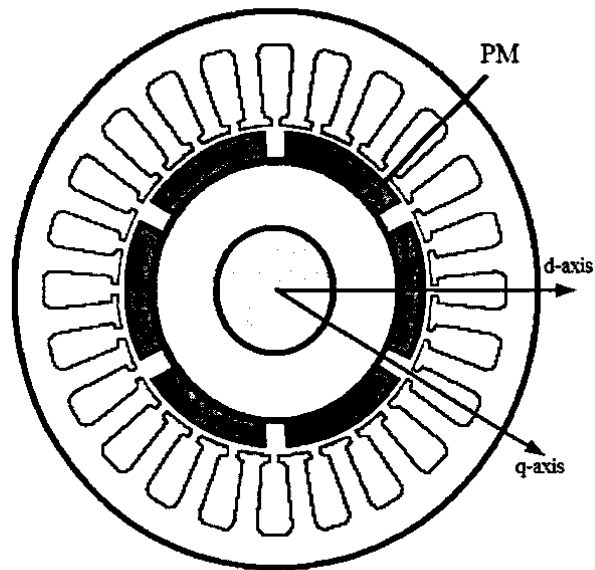
Figure 2.2: Cross-section view of SPMSM.

Another configuration in positioning the PM is called interior PMSM or IPMSM where the PM are buried inside the rotor and it is shown in Figure 2.3.
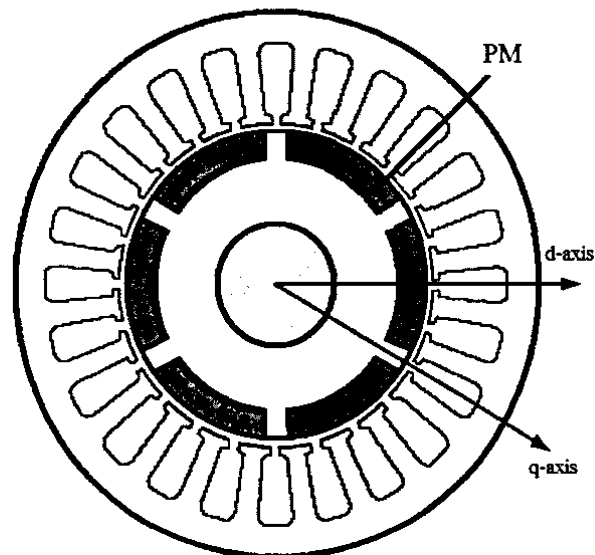
Figure 2.3: Cross-section view of IPMSM.

In this configuration the PMs are buried inside the rotor as mentioned, and this makes the effective air gap un-uniform, i.e. the effect of saliency appears here. It should be also noted that the rotor direct axis, d-axis is defined for the magnetic flux produced by the PMs through the centre line of the magnets, and the rotor quadrature axis, q-axis is displaced at 90 electrical degrees from the d-axis. This illustrates the saliency effect; since the relative permeability of the air is 1, and the permeability of the PMs is very close to 1, so the saliency effect in the case of SPMSM will disappear and make the q-inductance greater than the d-inductance.

2.2 Mathematical Model of the SPMSM

The mathematical model of the surface-mounted PMSM is reviewed here before proceeding to the controller and speed estimation of the motor. A detailed modeling of SPMSM is required for the simulation accuracy. The effect of iron losses, end-effects and saturation are neglected [5-27].

The voltage equations of PMSM in the rotor reference frame (d–q reference frame) -as shown in Figure 2.1- can be written as follow [5-10]:

$$v_d = R_s i_d + L_d \frac{d}{dt} i_d - \omega_e \lambda_q \tag{2.1}$$

$$v_q = R_s i_q + L_q \frac{d}{dt} i_q + \omega_e \lambda_d \tag{2.2}$$

Where:

v_d, v_q : the d and q-axis of the stator voltage.

R_s: The stator resistance.

i_d, i_q: the d and q-axis of the stator current.

ω_e: the rotor's electrical angular velocity.

λ_d, λ_q: the Stator Flux Linkages in d and q-axis.

And the Flux Linkages can be expressed as follow:

$$\lambda_d = L_d i_d + \lambda_m \tag{2.3}$$

$$\lambda_q = L_q i_q \tag{2.4}$$

Where:

λ_m: The Flux Linkage of the PM.

L_d, L_q: the d and q-axis stator inductance.

Substituting (2.3) and (2.4) in (2.2) and (2.1) respectively, the voltage equation is then expressed as follow:

$$v_d = R_s i_d + L_d \frac{d}{dt} i_d - \omega_e L_q i_q \tag{2.5}$$

$$v_q = R_s i_q + L_q \frac{d}{dt} i_q + \omega_e L_d i_d + \omega_e \lambda_m \tag{2.6}$$

The motor's developed torque is given by:

$$T_e = \left(\frac{3}{2}\right)\left(\frac{P}{2}\right)\left[\lambda_m i_q + \left(L_d - L_q\right)i_q i_d\right]$$

(2.7)

In the case of surface-mounted PMSM, the effective air gap is uniform and the effect of saliency is negligible. This means that the direct axis stator inductance equals the quadrature axis stator inductance, i.e. $L_d = L_q = L$. This leads to a simplified motor's developed torque equation and equation (2.7) can be rewritten as follow:

$$T_e = \left(\frac{3}{2}\right)\left(\frac{P}{2}\right)\left[\lambda_m i_q\right]$$

(2.8)

It is very clear from equation (2.8) that the developed torque of SPMSM depends only on the q-axis current since the PM flux linkage is constant.

Completing the mathematical model, the mechanical characteristics equation is

$$T_e = T_L + \beta \omega_m + J \frac{d}{dt}\omega_m$$

(2.9)

and

$$\omega_m = \left(\frac{2}{P}\right)\omega_e$$

(2.10)

$$\omega_e = \frac{d}{dt}\theta_r$$

(2.11)

Where:

T_L: the load torque.

13

β: the viscous friction coefficient.

J: the moment of inertia.

ω_m: the rotor mechanical angular velocity.

P: number of poles.

θ_r: The rotor position angle.

The d-q model of the motor can be easily transformed into a three-phase voltage equation and vice versa by using Park and inverse Park transformation. It can be also transformed into α-β reference frame by using Clark transformation [1].

2.3 SPMSM Operation

As mentioned previously, Synchronous machines got their name from the fact that its speed is directly related to the line frequency; the relationship that relates the speed of the motor and the electrical speed was shown in equation (2.10). It can be also rewritten as follow:

$$\omega_m = \left(\frac{2}{P}\right)\omega_e = \left(\frac{2}{P}\right)2\pi f$$

(2.12)

Where f is the line frequency.

A constant torque can be delivered by the motor while running the motor below the rated speed and taking into consideration that the output voltage and current of the inverter don't reach its limit. The induced back-EMF and the power will increase as the motor's

14

speed increases. When the PMSM runs at its base speed, then the induced back-EMF approaches the maximum terminal voltage of the inverter and it is clear that the torque will decrease as the speed of the motor increases.

The wide speed range operation of PMSM is the idea of running the motor below and above its base speed. Figure 2.4 shows the typical characteristics curve of Torque/Power vs. speed of PMSM. In order to extend the operating speed of the motor in the constant output power region, then the air-gap flux should be reduced or weakened while keeping the voltage at its maximum value.

Since the rotor's PM flux is constant, reducing the air-gap flux could be done by Field Weakening techniques. The Field weakening technique based on applying an appropriate amount of negative magnetizing current (field generating) component (i_d) to weaken the total air-gap flux and extend the PMSM's operating speed above the base speed. This method is restricted by the maximum allowable current and voltage of the inverter. A lot of work has been done in this field to utilize the inverter and achieve the field weakening control [9-11].

15
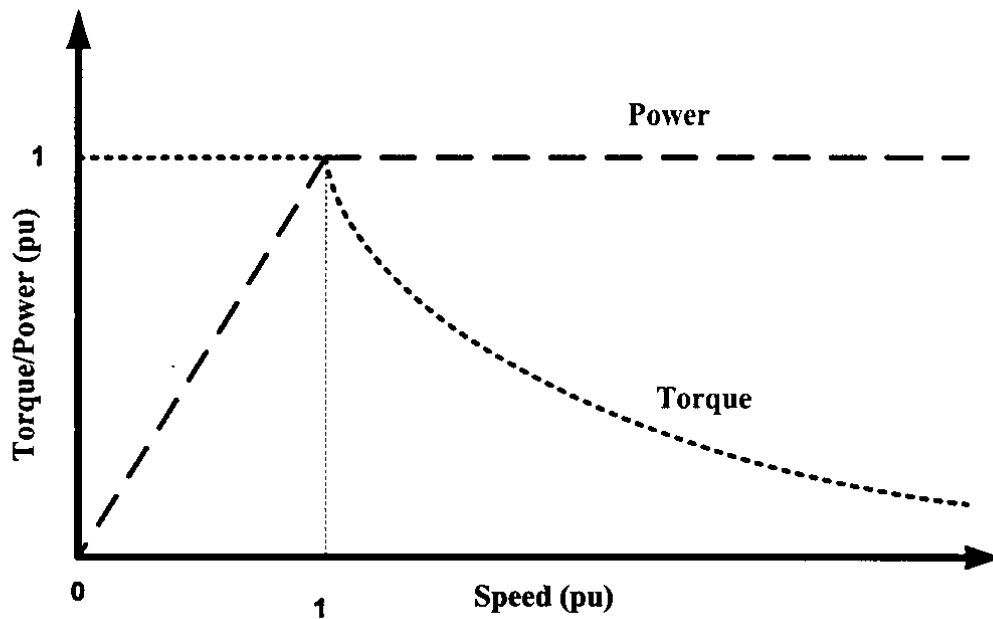
Figure 2.4: The Torque/Power vs. Speed characteristics.

2.4 Dynamic simulation of SPMSM

The mathematical model of the SPMSM is implemented in Matlab/Simulink in order to check the behavior of the motor at different speeds and torque levels. This Simulink model is used in the presented control technique. The structure of the Simulink model is shown in Figure 2.5.
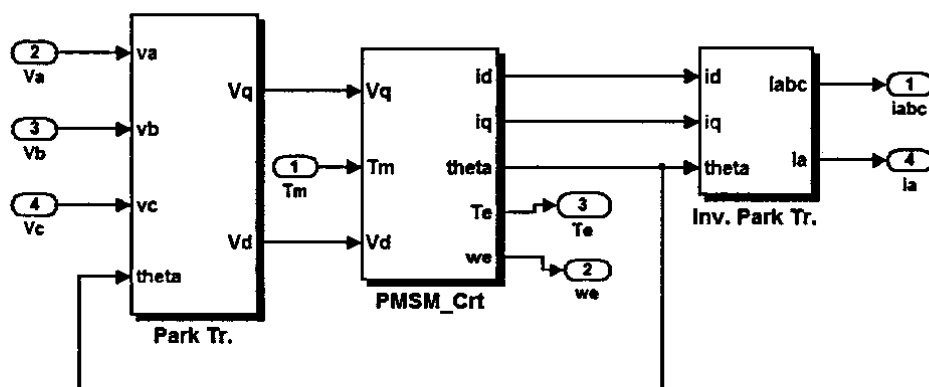
Figure 2.5: SPMSM simulation model.

16

The inputs to the simulation model are the three phase voltages Va, Vb, Vc and the mechanical load. These voltages are then transformed into d-q reference frame by using Park transformation shown in Figure 2.6 which requires the knowledge of the rotor position θ_r which can be calculated by (2.11). The outputs of the simulation model are the rotor speed and the three phase currents which have been transformed from d-q reference frame into a,b,c frame using inverse Park transformation as shown in Figure 2.7.
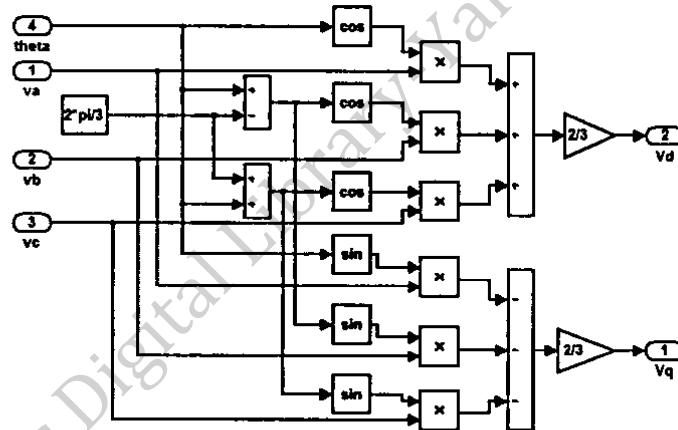
Figure 2.6: Park Transformation.
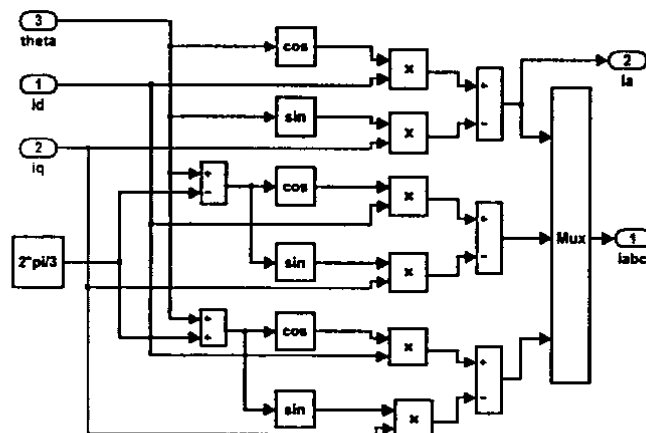
Figure 2.7: Inverse Park Transformation.

17

Inside the PMSM block, the d and q-axis currents, motor speed and torque where modeled using equations (2.5) – (2.11). The model is shown in Figure 2.8.
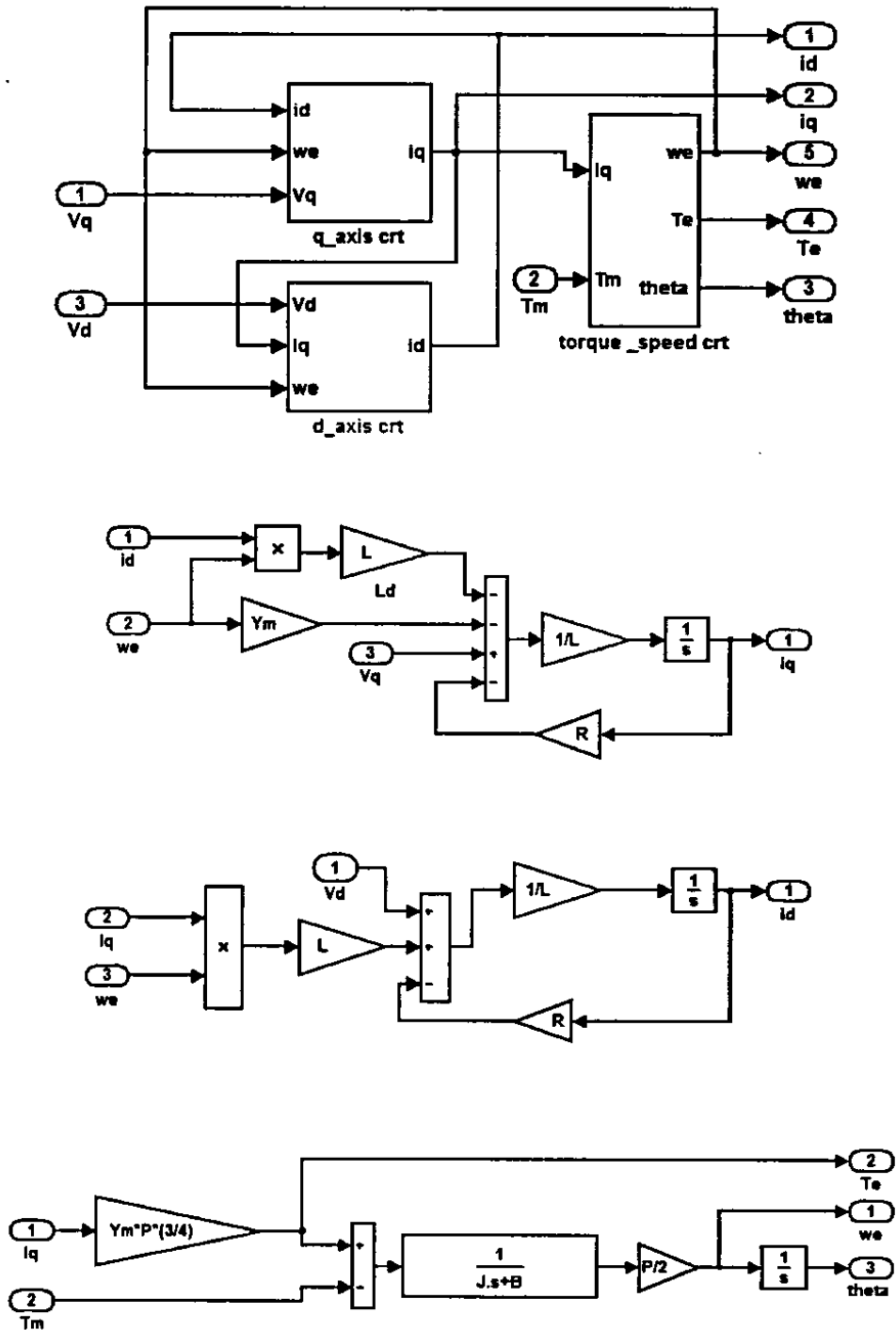
Figure 2.8: Currents, Torque and Speed Simulink blocks.

18

2.4.1   SPMSM Parameters

The SPMSM parameters used are listed in table 2.1 [35].

Table 2.1: SPMSM Parameters

The stator resistance Rs (Ω)	1.4
The stator inductance L (H)	0.0066
The PM flux λ_m (wb)	0.1546
Number of Poles P	6
J (kg.m^2)	0.00176
B (N.m.s)	0.00038818
T_n (N.m)	7
f (Hz)	50

2.4.2   SPMSM simulation results

The first test was done by supplying the SPMSM with a three phase voltage of 30 V phase amplitude and 5 Hz frequency, the Load was 2 N.m. The results are shown in Figures 2.9 - 2.11.

Figures 2.12 - 2.14 shows the response of the motor at 30 V amplitude phase voltage, 10 Hz frequency and increasing the load to 4 N.m. The simulation results show the accuracy of the built model since the response matches and verify the equations presented in this chapter.

19

Three-Phase voltages
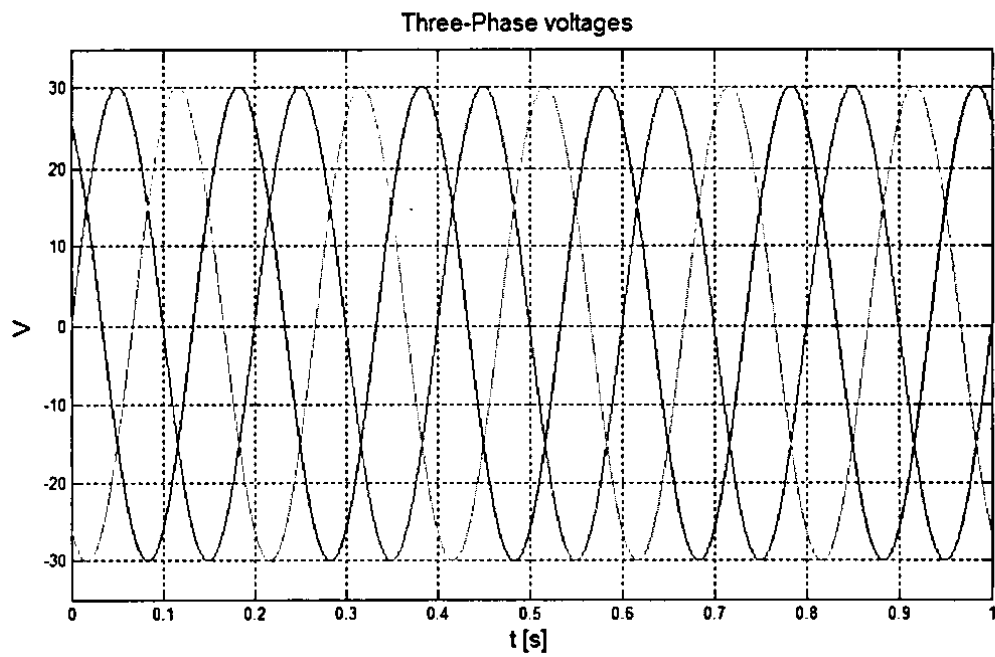
Figure 2.9: The three-phase voltage inputs to the motor at 5 Hz frequency.

Three-Phase Currents
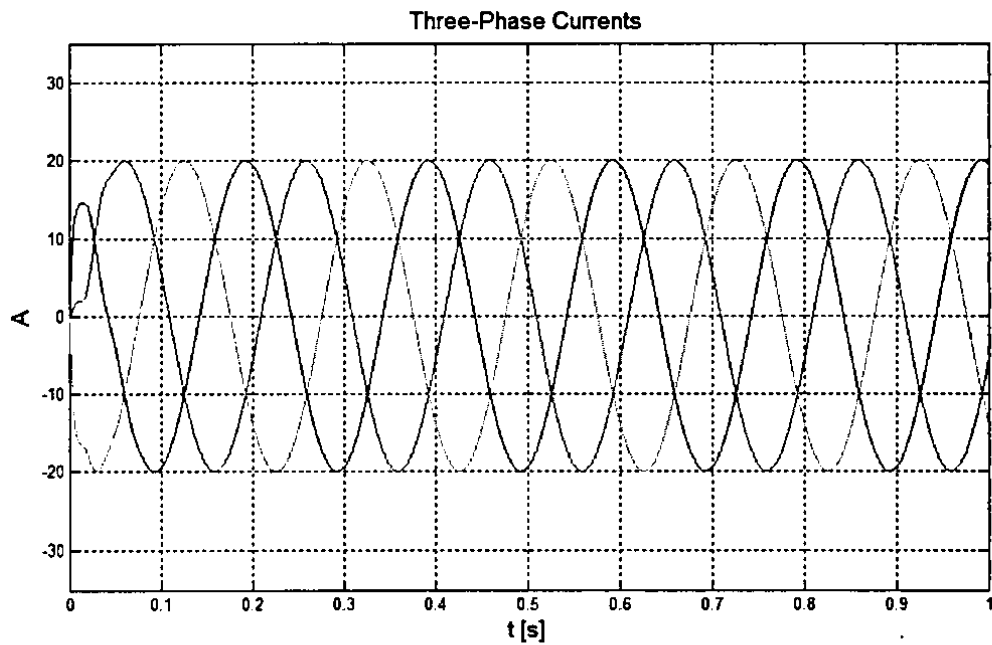
Figure 2.10: The Three-phase currents of the motor at 2 N.m load.

20
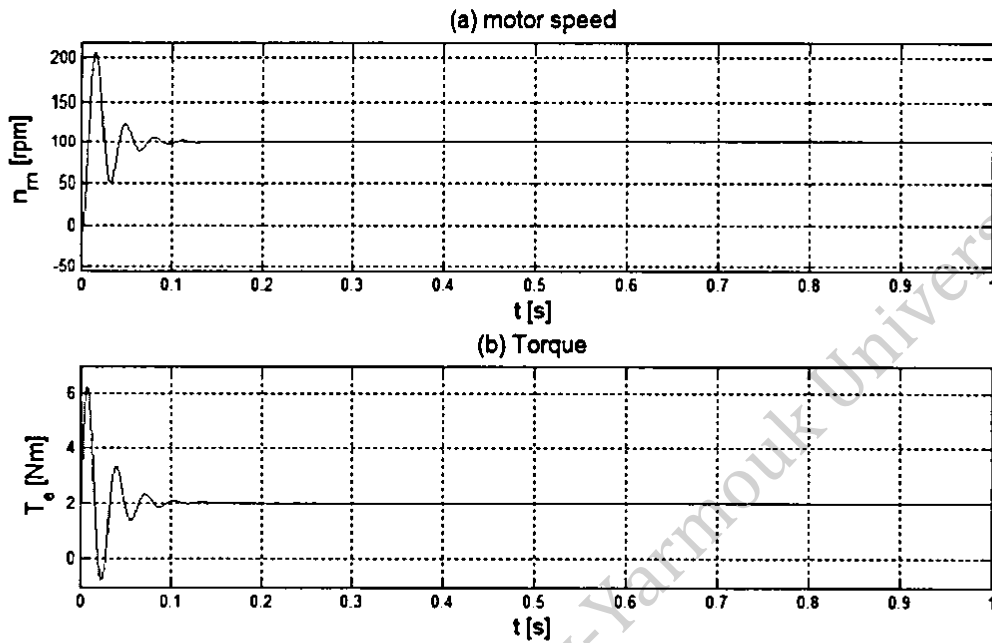
Figure 2.11: The motor Speed and Torque at 2 N.m load and 5 Hz frequency.
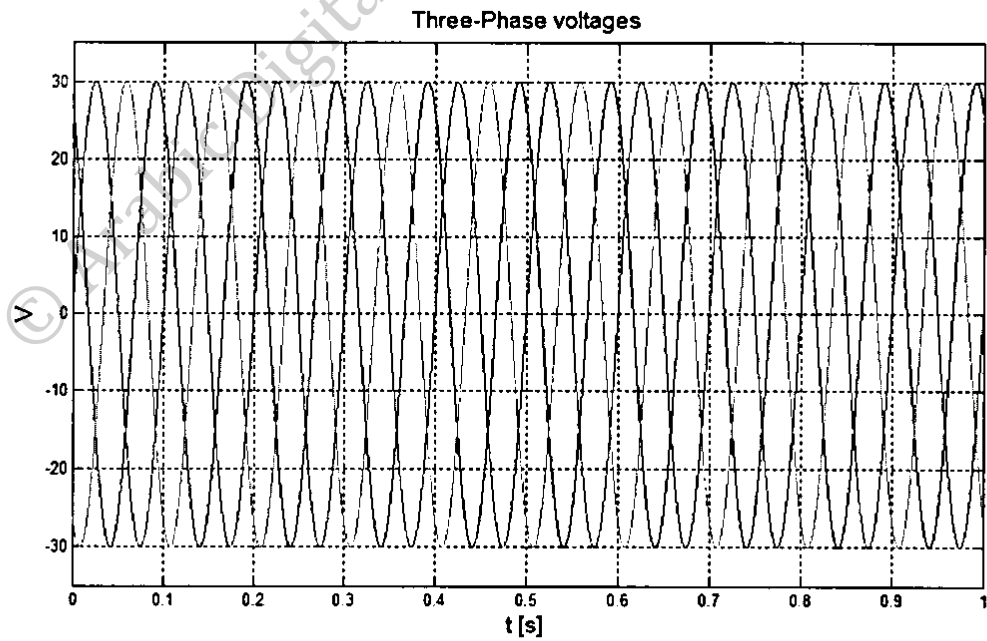
Figure 2.12: The three-phase voltage inputs to the motor at 10 Hz frequency.

21
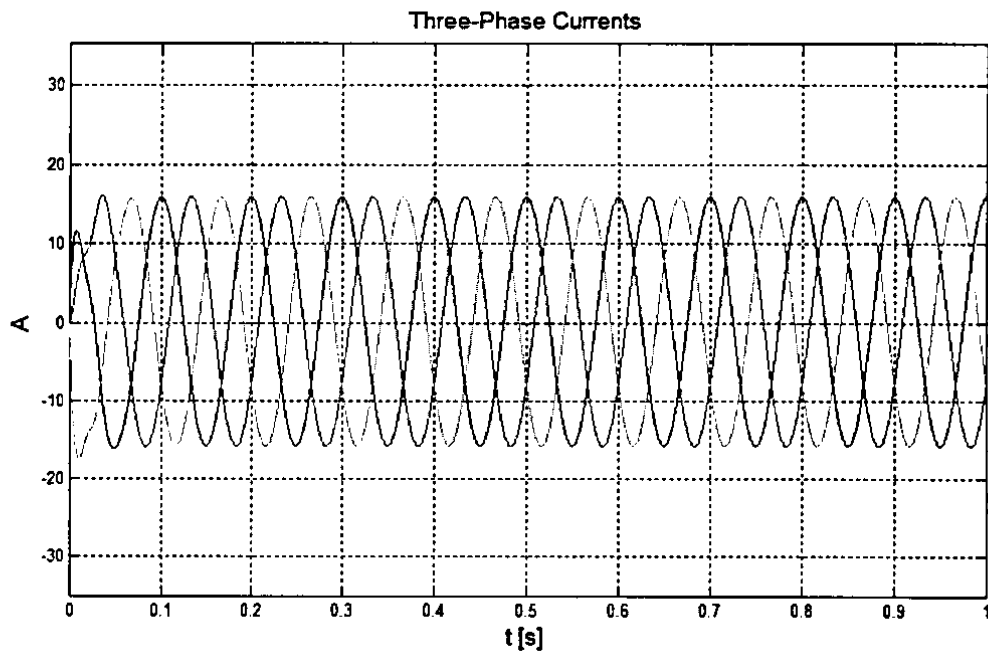
Figure 2.13: The Three-phase currents of the motor at 2 N.m load.
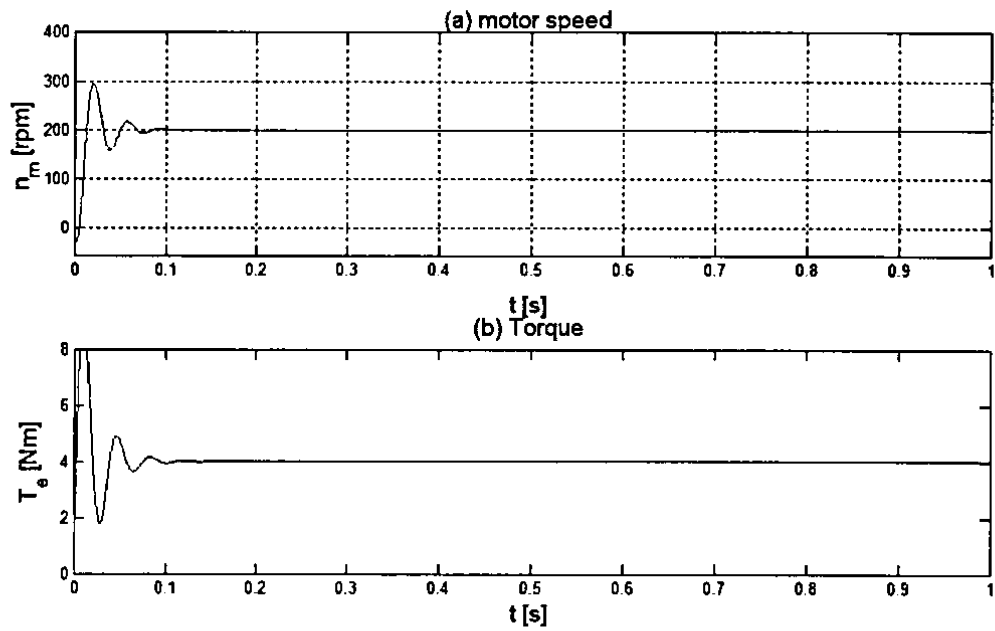
Figure 2.14: The motor Speed and Torque at 4 N.m load and 10 Hz frequency.

22

2.5 SPMSM Control

In general, the key factor in controlling the PMSM is accurate current regulation; i.e. controlling the i_d and i_q current components independently. This control scheme enables the control of torque and flux simultaneously. The rotor flux is oriented with the direct axis and decoupling the current components so they can be controlled in both magnitude and phase angle. Decoupling the current components means that the torque and flux are decoupled too and can be controlled independently. This is because the Torque is proportional to the q-axis current component and the flux is directly related to the d-axis current component. Figure 2.15 shows a general block diagram of SPMSM control.

Figure 2.15: General Block Diagram of UPFC of SPMSM.

Control of PM motors is performed by using a Pulse Width Modulation (PWM) inverter and decoupling control to get the dynamic performance of PMSM to be similar to that of DC motors. The stator windings of the motor are fed by an inverter that generates variable

output voltage and frequency. It is clear also that the rotor position is required for accurate orientation control of the motor. If the rotary encoder is replaced with an algorithm to calculate and estimate the rotor speed and position; then this drive system is referred to as a sensorless drive system which will reduce the cost and increase the reliability of the overall drive system.

Chapter 3 UNITY POWER FACTOR CONTROL OF PERMANENT MAGNET SYNCHRONOUS MOTORS

In this chapter, a unity power factor control scheme of PMSM is studied. Based on a current control concept, a new UPF controller is developed and modeled and the phasor diagram for the currents trajectories are also illustrated in the rotor reference frame. A review of the used Voltage Source Inverter (VSI) is presented too; the simulation model is designed by using Matlab/Simulink software.

3.1 Power Factor Definition

The Power Factor (PF) is an indicator or a measure of how the current is being effectively converted into a useful output work. It is defined as the ratio between the real power and the apparent power drawn by an electrical load. It is simply defined as follow [3, 4]:

$$PF = \frac{Real\ Power}{Apparent\ Power} = \frac{P}{|S|} \tag{3.1}$$

In order to follow up with the unity power factor control system of PMSM, it is more convenient to review the AC power components that flows throw an electrical load. The first component is the Real Power (P), it is also called the Active Power or Average Power and it is measured in watts (W). The second component is the Apparent Power (S) and it is

25

measured in Volt-Amperes (VA). The final one is the Reactive Power (Q) which is measured in Volt-Ampere Reactive (VAR).

Practical loads have a resistance, inductance and/or capacitance components. When an AC voltage is being applied to a resistive load, then there is no phase difference between the voltage and current and hence ϕ equals zero - the phase difference or phase shift symbol will be considered as ϕ -. The power consumed in the resistive load will be only a real power in which a useful work has been transferred to the load.

In case of an inductive load; when the voltage is applied, then it will resist the change in the current which yields the current to lag the voltage and a phase difference will appear between the voltage and current by 90°. The case is different in a capacitive load where the current will lead the voltage by 90° and a reactive power Q will be consumed.

Figure 3.1 shows the Power triangle of an AC load in which the voltages and currents are assumed to be sinusoidal. The power components then can be expressed as vectors such that:

$$S^2 = P^2 + Q^2 \tag{3.2}$$

Where

$$P = |S|\cos(\phi) \tag{3.3}$$

$$Q = |S|\sin(\phi) \tag{3.4}$$
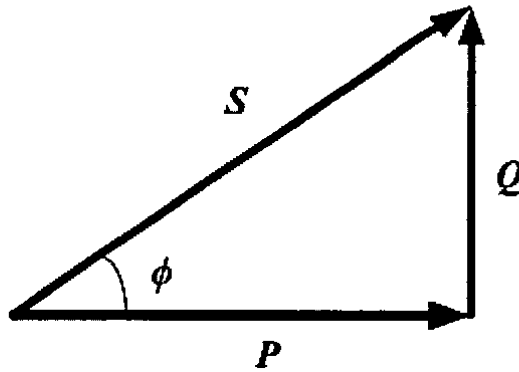
Figure 3.1: The Power Triangle

By substituting (3.3) into (3.1), then the power factor will be redefined as follow:

$$PF = \cos(\phi) \tag{3.5}$$

According to the above expression, the power factor will take ranges from 1 to 0 and it is important to mention that the reactive power consumed by reactive loads does not transfer energy to the load; it only will heat the electric wires and increase the losses. From this point, the Importance of a unity power factor control appears. In the case of PMSM drive systems, if the power factor is less than one, then the motor will draw more current for a given amount of power. So the UPFC will reduce the VA rating of the Voltage-Source Inverter VSI supplying the PMSM [5-8].

3.2 PMSM Control Techniques

PMSM can be controlled using two different control systems; scalar and vector control. The scalar control of PMSM is simple and derived from the steady state characteristics of the motor. In this category; only the magnitude of the controlled variable or the frequency is

27

being controlled. The transient response is very poor compared with that of DC motors. The second control system is the vector control which is superior to scalar control in which the state variables are controlled in both magnitude and angle (position). This system takes into consideration the transient response of the motor and guaranties a good transient and steady state response of the motor.

In vector control, the motor differential equations are transformed into a decoupled d-q coordinate system which rotates synchronously with the PM flux. The decoupling control will allow a separate control of speed, torque and flux just like that of DC motors by mean of controlled current loops with PI regulators. The Unity Power Factor control or any other control techniques of PMSM could be achieved with vector control by separately controlling the d-q components of the stator current resulting in a high performance drive system. The control techniques of PMSM are listed bellow [8]:

• Unity power factor control (UPFC).

• Maximum torque per ampere control (MTPAC).

• Constant torque angle control (CTAC).

• Constant stator flux control (CSFC).

In MTPAC strategy; minimum stator current amplitude is needed to develop the torque. In the case of SPMSM, this control strategy is done by controlling i_d current to be zero. This will reduce the losses and increase the efficiency of the motor.

CTAC is achieved by controlling the torque angle between the stator current vector and PM flux at constant value which is 90°. Comparing it with the MTPAC of SPMSM drives;

there is no difference between these two control techniques since both require keeping id current to zero. The control technique will be different in the case of interior type PMSM.

The constant stator flux control technique is based in controlling the amplitude of the stator flux linkage to be equal to the PM flux linkage. This control technique has the advantage of keeping the power factor very close to 1. While the UPFC technique ensures that the power factor is exactly 1.

3.3 Unity Power Factor Control (UPFC) of PMSM

The purpose of UPFC is to keep $\cos(\phi)$ equals one; i.e. the angle between the voltage and current of the motor is zero ($\phi=0$) which means that they are in phase. This could be done by controlling the d axis current of the PMSM. It can be proved by the following set of equations:

The stator voltage of the motor v_s is expressed as follow:

$$vs = \sqrt{vd^2 + vq^2} \angle \tan^{-1}\frac{vq}{vd} \tag{3.6}$$

And the stator current of the motor i_s is expressed as follow:

$$is = \sqrt{id^2 + iq^2} \angle \tan^{-1}\frac{iq}{id} \tag{3.7}$$

So the condition of unity power factor operation of the motor is that the current angle should equal the voltage angle; such that there is no phase shift between them. The voltage angle in (3.6) should equal the current angle in (3.7), then:

$$\frac{iq}{id} = \frac{vq}{vd}$$

(3.8)

The reference direct axis current that ensure the unity power factor operation of the Surface-mounted PMSM is [5]:

$$id = iq\frac{vd}{vq}$$

(3.9)

Equation (3.9) which has been used in [5] requires stator currents and voltages sensors to calculate the reference d-axis current (i_d). While the new system for calculating the reference i_d current presented in this thesis requires only a current sensor to measure i_q current component without the need to measure the stator voltages. This new technique is simple and reduces the system complexity. The next paragraph shows how to calculate the reference i_d for the unity power factor operation of surface-mounted PMSM.

In order to calculate the reference i_d, the steady state equations of the motor voltages should be analyzed. The motor dynamic model presented in chapter two is repeated here for convenience:

$$v_d = R_s i_d + L\frac{d}{dt}i_d - \omega_e L i_q$$

(2.5)

$$v_q = R_s i_q + L\frac{d}{dt}i_q + \omega_e L i_d + \omega_e \lambda_m$$

(2.6)

At steady state; equations (2.5) and (2.6) will be as follow:

$$V_d = R_s I_d - \omega_e L I_q \tag{3.10}$$

$$V_q = R_s I_q + \omega_e L I_d + \omega_e \lambda_m \tag{3.11}$$

Where the capital letters represent the steady state values of currents and voltages.

By substituting (3.10) and (3.11) into (3.9):

$$I^*_d = I_q \frac{R_s I_d - \omega_e L I_q}{R_s I_q + \omega_e L I^*_d + \omega_e \lambda_m} \tag{3.12}$$

$$I^*_d \left(R_s I_q + \omega_e L I^*_d + \omega_e \lambda_m \right) = I_q \left(R_s I^*_d - \omega_e L I_q \right) \tag{3.13}$$

$$R_s I_q I^*_d + \omega_e L I^{*2}_d + \omega_e \lambda_m I^*_d = R_s I^*_d I_q - \omega_e L I^2_q \tag{3.14}$$

Now the term $R_s I_q I^*_d$ will cancel each other in both side of equation (3.14), then:

$$\omega_e L I^{*2}_d + \omega_e \lambda_m I^*_d = -\omega_e L I^2_q \tag{3.15}$$

Dividing (3.15) by $\omega_e L$ and arranging it, we will get the following equation:

$$I^{*2}_d + \left(\frac{\lambda_m}{L} \right) I^*_d + I^2_q = 0 \tag{3.16}$$

Solving this quadratic equation in terms of i_d and taking into consideration that i_q is constant here and it depends only on the load as it is clear from equation (2.8); The reference i_d that ensures the UPF operation is then:

31

$$I^*_d = \frac{-\left(\lambda_m/L\right) + \sqrt{\left(\lambda_m/L\right)^2 - 4(I_q)^2}}{2}$$

(3.17)

It is clear from (3.17) that only the quadrature axis current is required to estimate the reference direct axis current. This will reduce the cost of the drive system since only one current sensor is required. It should be noted that in (3.17) when i_q is very high during transient response; then the value under the square root will be negative and the reference I_d current will be complex; so only the real part of I_d should be considered.

The space vector diagram of SPMSM under UPF operation is shown in Figure 3.2. In this case, the advantage of UPFC comes from the fact that only real power is being supplied to the motor and so the VA rating of the inverter is reduced.

It is clear from Figure 3.2 that the stator voltage and current are in phase and ϕ equals zero. The PM flux vector λ_m is located in the d-axis and its magnitude is constant. It is clear that the value of the i_d is always negative as shown in equation (3.17). Furthermore; i_q is constant at any speed reference, it depends only on the electromechanical torque of the motor.

q-axis
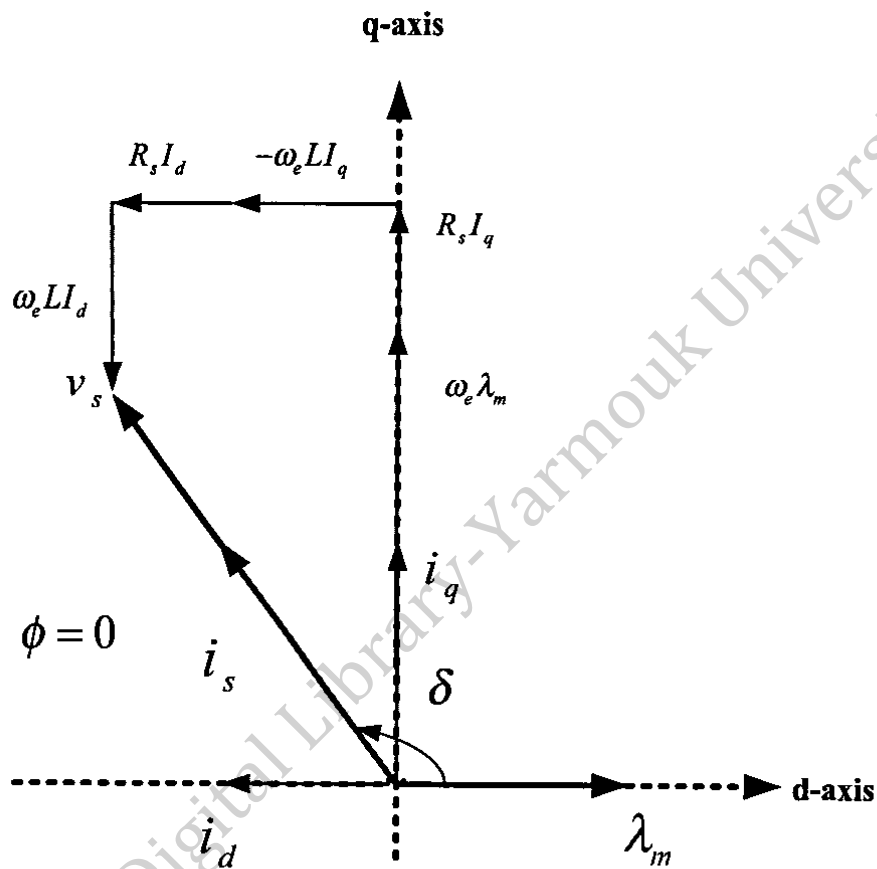
Figure 3.2: Current and Voltage vectors under UPFC.

Figure 3.3 shows the block diagram of UPFC of SPMSM. The stator currents and voltages are then transformed into d-q reference frame by doing Park transformation to get the actual values of i_d, i_q, v_d and v_q. This model uses equation (3.9) to calculate the reference (command) value of the d-axis current. This value is then compared with the d-axis stator current measured from the SPMSM and forcing it to follow up this reference value by mean of a PI controller.
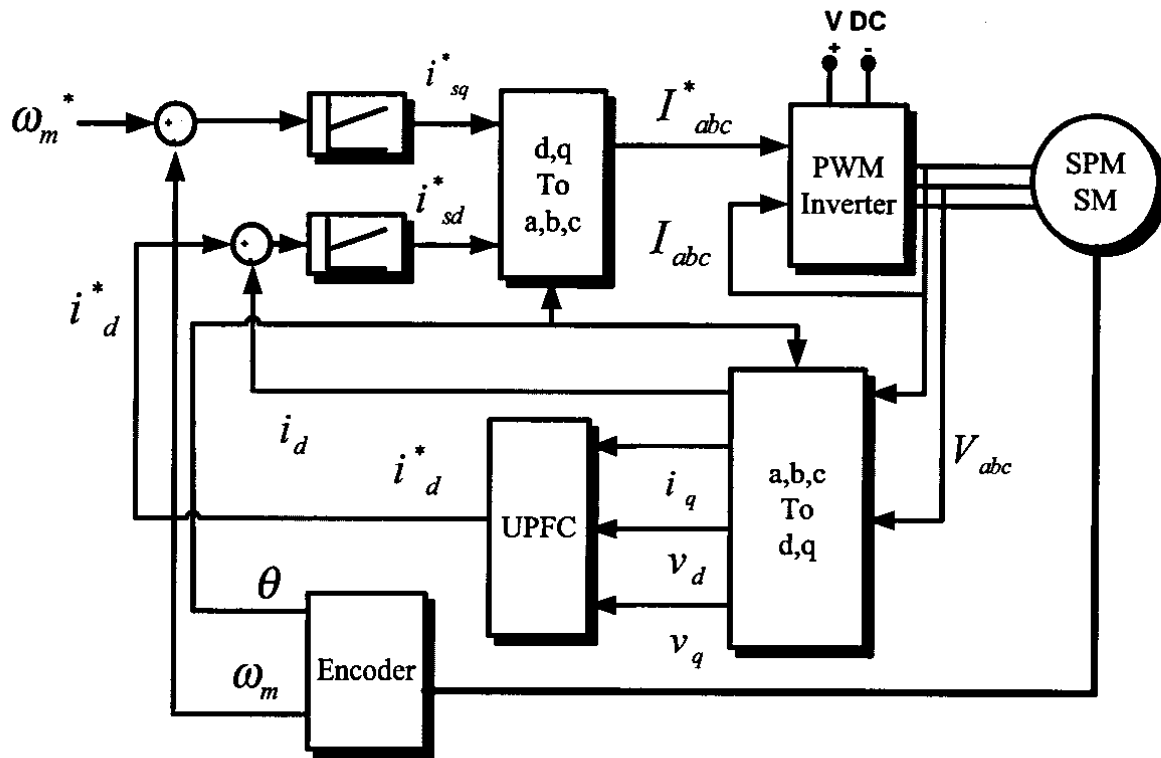
Figure 3.3: Detailed block diagram of UPFC of SPMSM.

The model shown in Figure 3.3 can be simplified as mentioned above by considering equation (3.17) for calculating the reference i_d value. Figure 3.4 shows the new simplified model based on equation (3.17) and it is clear that only a current sensor is required for the UPF controller.
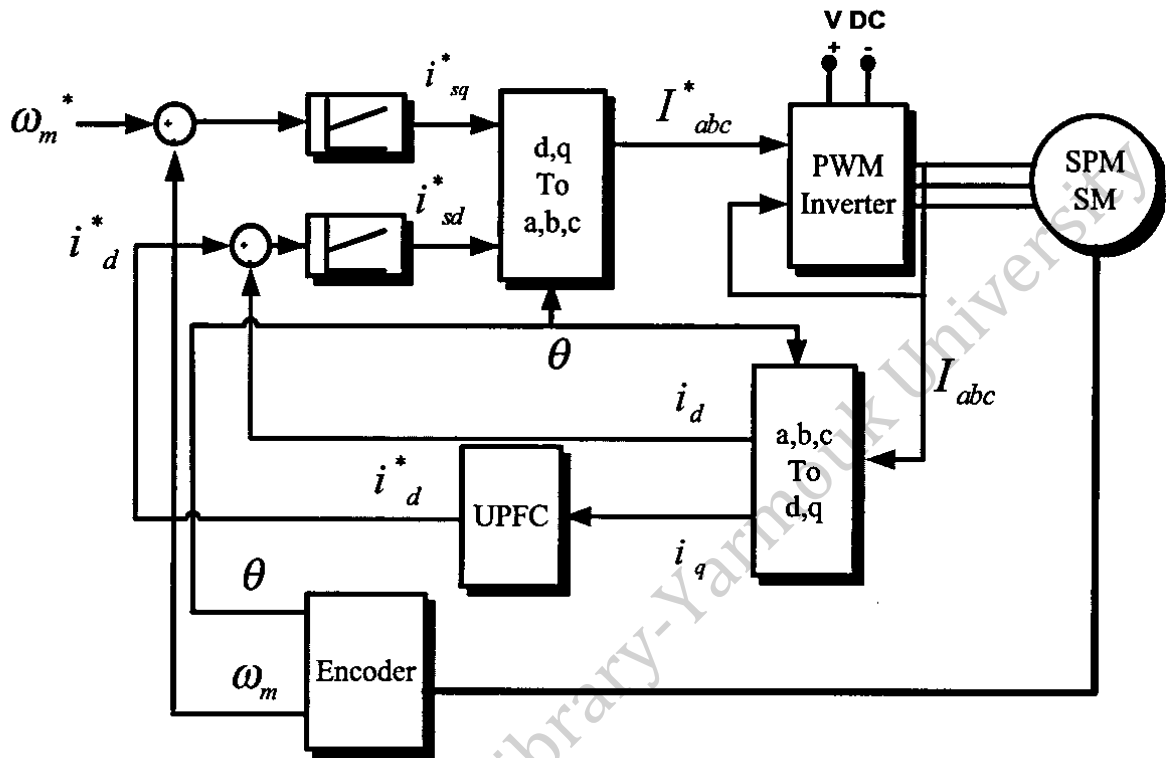
Figure 3.4: The block diagram of the new UPFC of SPMSM.

3.4 Stator currents and voltages limitations Under UPFC

As shown in the control system of UPFC in Figure 3.4, the SPMSM is fed by a PWM Voltage Source Inverter (VSI). The output voltage of the VSI is varied according to the speed of the SPMSM. When the speed of the motor is increased; then the output voltage of the VSI should be increased to keep the value of the stator current required by the torque production. This output voltage has a limit determined by the VSI.

35

Furthermore; the maximum stator current of the SPMSM is also limited by the VSI and the motor itself. This will limit the maximum output torque of the motor since it depends on the stator current.

Considering the voltage and current constraints of the VSI and SPMSM; let us assume that the VSI output voltage reaches its limit, which is V_{smx}. Then the voltage constraint should satisfy the following equation:

$$V_d^2 + V_q^2 \leq V_{smax}^2 \tag{3.17}$$

This equation represent a circle centered at (0,0) and with radius V_{smax}. Substituting (3.10) and (3.11) into (3.17), then:

$$(R_s I_d - \omega_e L I_q)^2 + (R_s I_q + \omega_e L I_d + \omega_e \lambda_m)^2 \leq V_{smax}^2 \tag{3.18}$$

Since the concentration now on high speed operation of the motor which requires high value of VSI output voltage, then the assumption of neglecting the voltage drop of the stator resistance is valid at high speed. Equation (3.18) will be then as follows [9-11]:

$$(-\omega_e L I_q)^2 + (\omega_e L I_d + \omega_e \lambda_m)^2 \leq V_{smax}^2 \tag{3.19}$$

By arranging the above equation, then

$$(I_q)^2 + (I_d + \frac{\lambda_m}{L})^2 \leq (\frac{V_{smax}}{\omega_e L})^2 \tag{3.20}$$

Equation (3.20) represents a circle equation on the $i_{d\text{-}q}$ coordinate plane. The center of this circle is (0, λ_m/L) and the radius is ($V_{smax}/\omega_e L$). This circle represents the stator voltage circle in the $i_{d\text{-}q}$ coordinate plane. When the motor is operating in the constant torque region,

36

and assuming that the VSI output voltage doesn't reach its limit; then when the speed of the SPMSM increases, the VSI voltage will increase too, but of course it will be much smaller that the motor speed. This means that as the motor speed increases; the radius of the voltage circle decreases. This operation is illustrated in Figure 3.5.
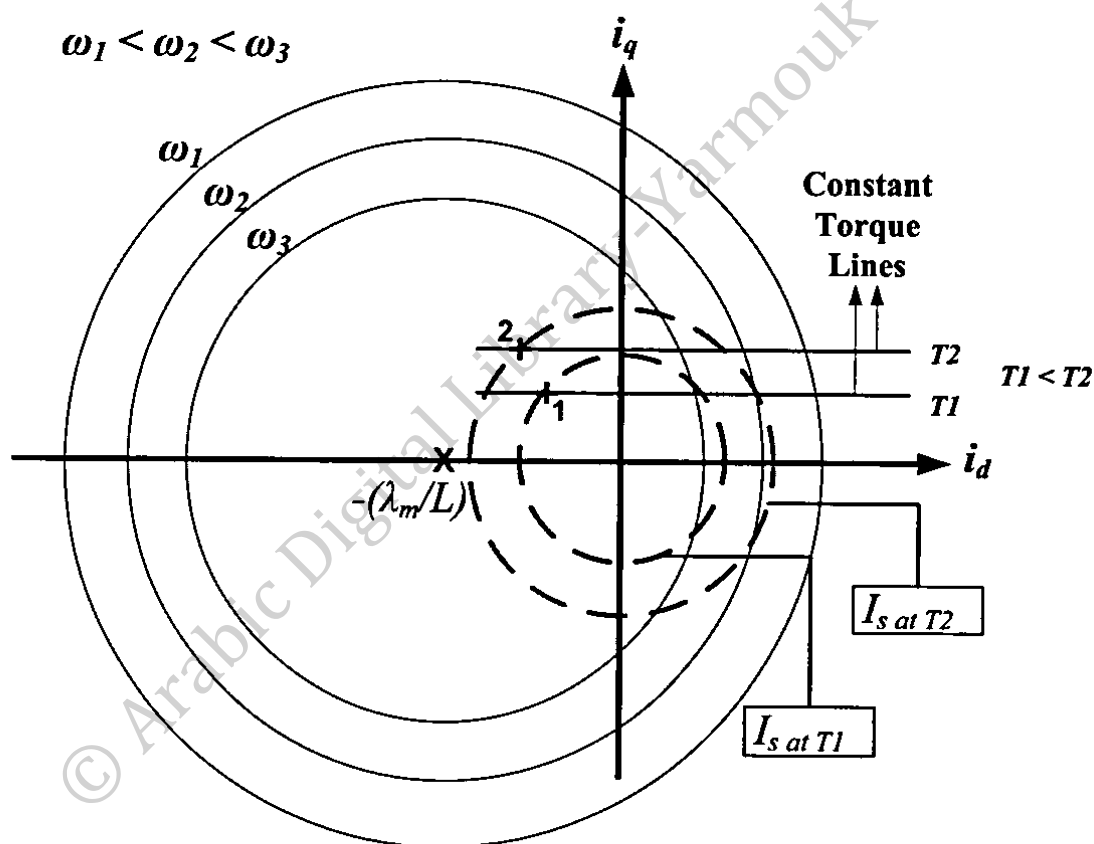
Figure 3.5: Voltage and Current circles of SPMSM.

It is clear from Figure 3.5 that the voltage limit circles (solid circles) shrink as the motor speed increases. The current circle (dashed circles) will not change since it depends only on the electromagnetic torque of the motor.

Let us assume that the motor is operating under torque value of T_1; the motor then will develop a constant value of i_q current and so on for i_d as in (2.8) and (3.17). The values of i_q and i_d will remain constant for different values of motor speed (point 1 in Figure 3.5). Let us then assume that the motor torque is then increased to a value of T_2; it is clear that i_q will increase and so for i_d (point 2 in Figure 3.5). It should be noted that the operating points 1 and 2 should be inside the voltage and current circles for constant torque operation of the motor. If the voltage limit circle largely shrinks (speed greater than the base speed) and the operating point of the motor became outside it; then this control system will not be able to drive the motor correctly and the Field Weakening Control technique should instead drive the motor in the constant power region where the motor developed torque will be reduced.

3.5 Three-Phase Voltage Source Inverter

The inverters are DC-to-AC converters where their function is to convert the DC input voltage into AC output voltage. The frequency and the amplitude of this AC output voltage are controllable. The DC input voltage of the VSI is fixed and not controllable. On the other hand, a variable output voltage is obtained using PWM techniques in order to change the gain of the inverter.

Three-phase VSI uses six controlled turn-on and turn-off power devices such as transistors and insulated-gate bipolar transistors (IGPTs). The configuration of the three phase inverters is shown in Figure 3.6. By switching the controlled power devices ON and OFF; a negative or positive DC voltage is applied to the motor's phases of variable frequencies and magnitudes; this is what called PWM.

38
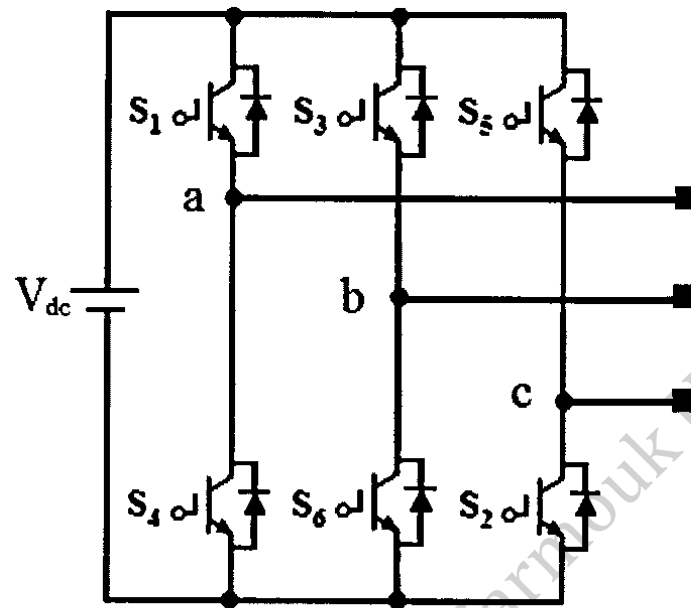
Figure 3.6: Three-Phase VSI.

The PWM technique used in this work is called Sinusoidal PWM or SPWM. The function of the SPWM is to generate the gating signals which switch the power devices on and off.

Figure 3.7 shows how the gating signals are generated with SPWM. There are three sinusoidal reference signals (V_{ra}, V_{rb} and V_{rc}). The amplitude of these reference signals is A_r and their frequency is f_r. They are also shifted by $120°$. The three sinusoidal reference signals are compared with a triangular wave signal (V_t). The amplitude of this triangular signal is A_t and its frequency is f_t which represents the PWM frequency. The amplitude and frequency of the triangular signal are fixed while the amplitude and the frequency of the three sinusoidal reference signals are variable. V_{ra}, V_{rb} and V_{rc} provide the gating signals for (S1, S4), (S3, S6) and (S5, S2), respectively.
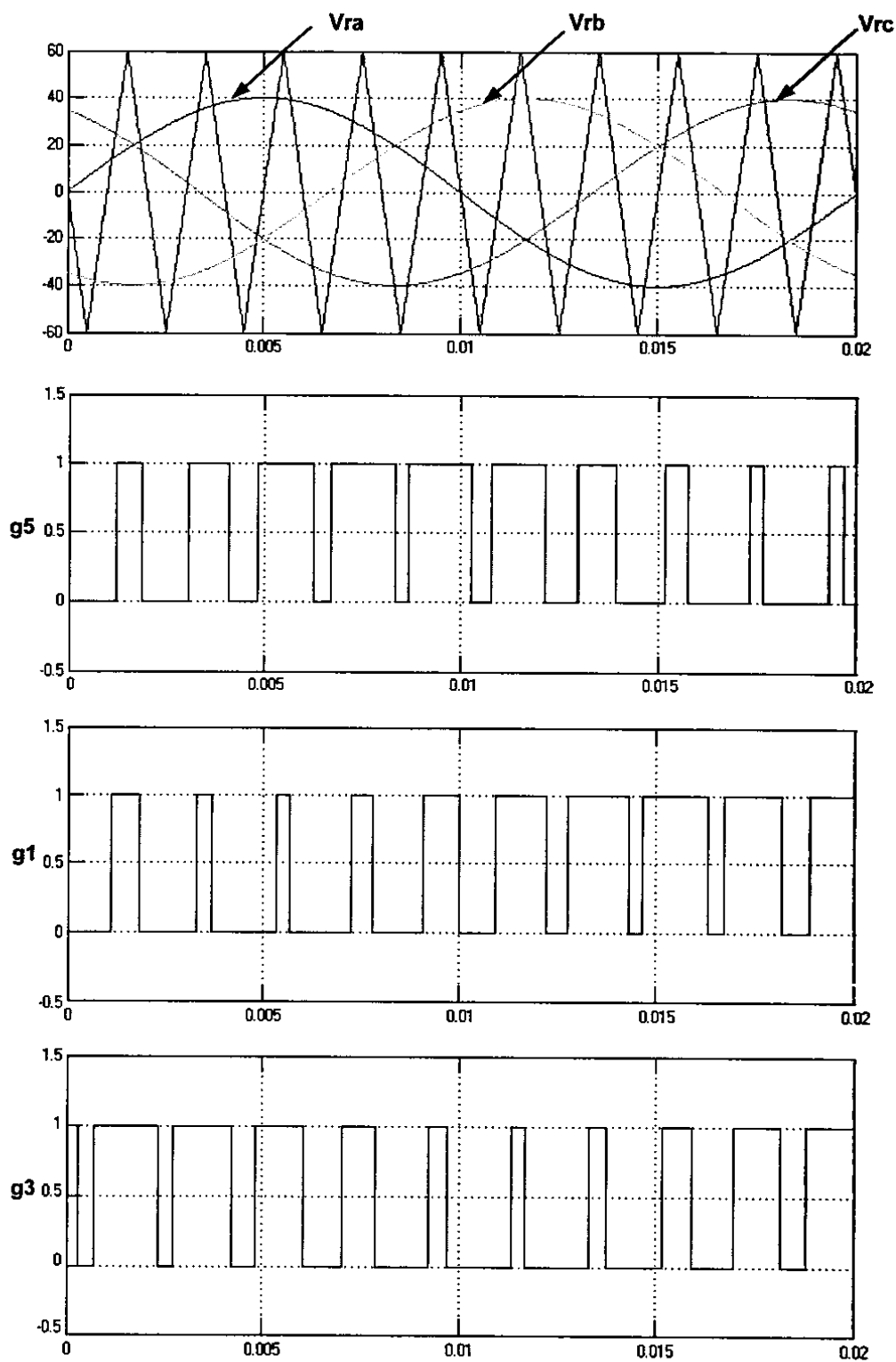
Figure 3.7: SPWM of three-phase inverter.

40
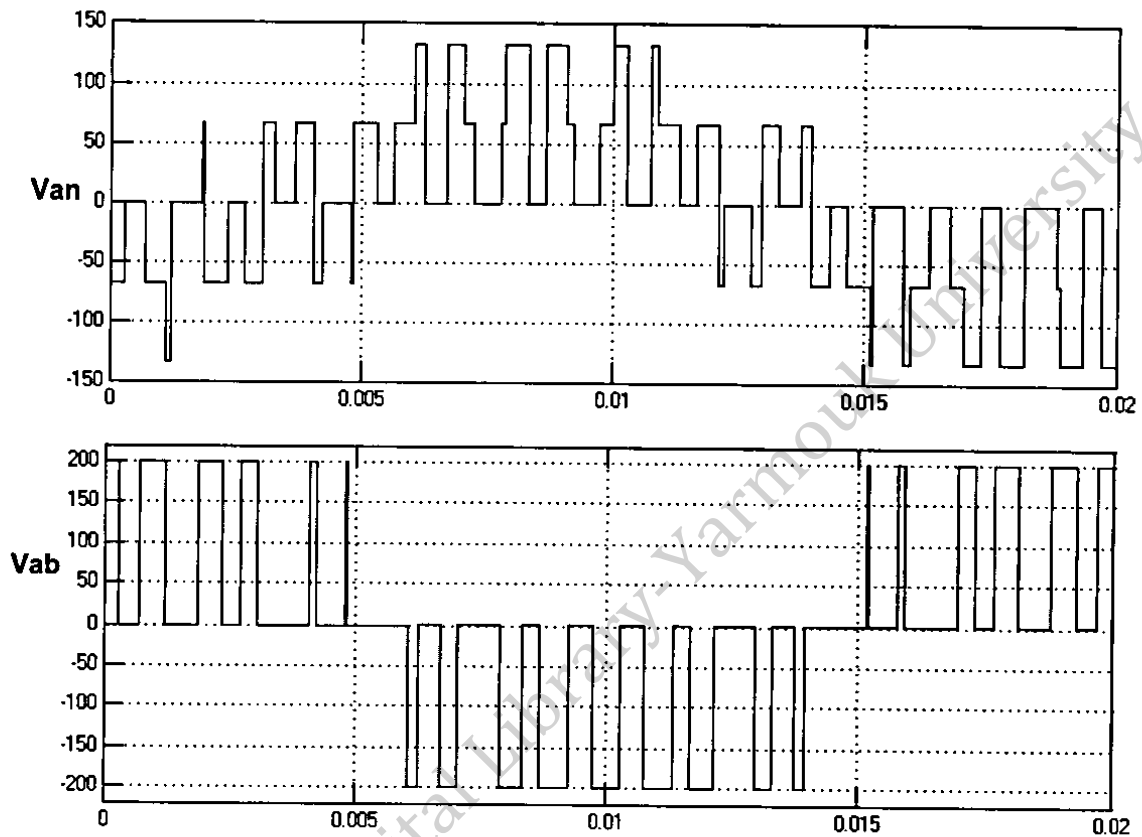
Figure 3.8: The phase and Line-to Line output voltage of the inverter.

The gating signals are produced using a comparator as mentioned above. When the triangular wave signal is greater than the sinusoidal reference signal, then the upper power switch is ON; on the other hand, the corresponding lower power switch is OFF in order to avoid the short circuit on the motor phase. The instantaneous Line-to-Line voltage is $V_{ab} = V_{dc} (g_1 \text{-} g_3)$. It is clear from Figure 3.7 that the inverter output frequency is directly related to the frequency of the three sinusoidal reference signals f_r, and the rms output voltage is directly related to the Modulation index. The peak amplitude A_r of the three sinusoidal

41

reference signals determines the modulation index which can be defined as in Equation 3.21 [1]:

$$M = (A_r / A_t)\qquad\qquad(3.21)$$

The three sinusoidal reference signal are provided from the motor stator currents as it is clear from Figure 3.4 where the input to the PWM inverter are the reference three-phase stator current (outputs of the PI controllers and noted as I^*_{abc} in Figure 3.4) and the three-phase stator currents measured from the motor (I_{abc} as in Figure 3.4). These two signals are then subtracted from each other and compared with the triangular wave signal. This is shown in Figure 3.9. The SPWM VSI can be treated as an amplifier; the gain of the inverter is [1]:
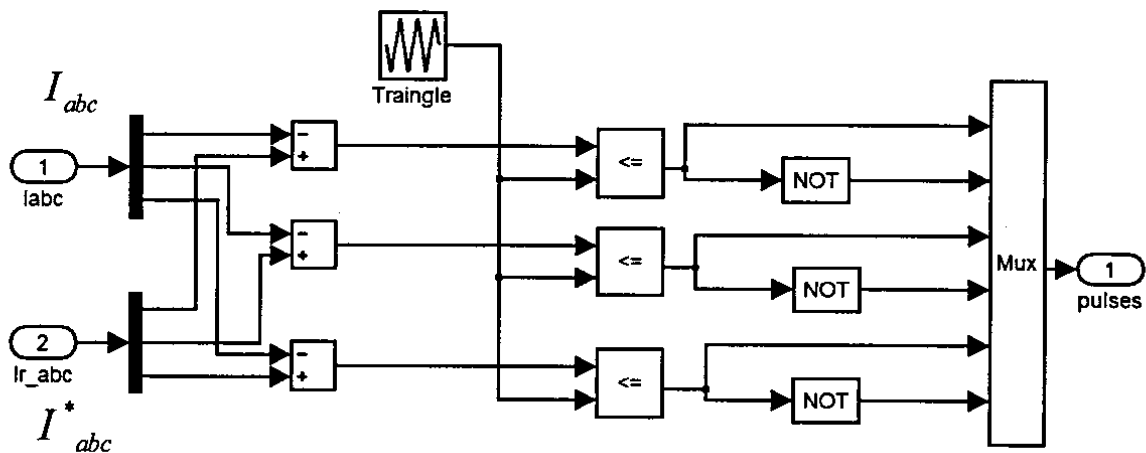
$$Gain = (0.5M\, V_{dc}) / A_r\qquad\qquad(3.22)$$

Figure 3.9: Gating circuit of SPWM VSI.

Chapter 4 SPEED SENSORLESS CONTROL OF PMSM

In this chapter, a speed and position sensorless control of SPMSM is developed. Based on the MRAS; a speed estimation is modeled and modified using Fuzzy Logic Controller. The simulation model was designed using Matlab/Simulink software.

4.1 Introduction

The position and speed sensor reduction in controlled drive systems is a major demand to increase the robustness and reliability of the drive system and reduce the overall cost [16-27]. Many techniques have been developed and implemented in the field of position estimation of the rotor. The rotor position is required in Vector Control of PMSMs drive system to compare the estimated speed with the reference speed in traditional PI or FLC. Many speed estimation methods based on the measured currents and voltages of the PMSM were developed. This can be achieved by measuring the stator currents or voltages [16], or calculating the stator flux to estimate the rotor position [17]. Another approach is by measuring the back EMF that is function of the rotor position [18]. A MRAS can be used to estimate the rotor position [19].

Regarding the sensorless technique and among all the different methodologies of estimating the rotor speed and position, the Sliding Mode Control (SMC) concept is better for robustness against disturbances and parameter variations [20-26]. The SMC uses a sign-

١

function of the estimated error as a feedback correction. A comparison between using the sliding mode concept and Fuzzy Logic will be shown in this chapter.

A reference model that contains the desired mathematical model and an adaptive model is used to adapt the reference model are used in the MRAS. The rotor speed is generated from the adaptation mechanism using the error between the estimated quantities obtained by the two models.

4.2 Model Reference Adaptive System

The MRAS is used in many different control systems and applications. It is used also in sensorless control systems to estimate the rotor speed of ac machines. MRAS takes advantage of a reference system model which provides the required performance specification that should be followed.

The General block diagram of MRAS (shown in Figure 4.1) uses two models; the reference model and the adjustable model for motor speed estimation. The MRAS estimates the same state variable y by using two different machine models, where y denotes the actual or correct values of the state variable and y^* is the estimated state variable where the rotor speed is used as a tuning signal which included in y^* estimation; i.e. the reference model tells the adjustable model how to respond to the input signal –the input signals are the stator current and voltages- by minimizing the error $(y-y^*)$ to zero. The adjustment mechanism is used to minimize the error signal.

44
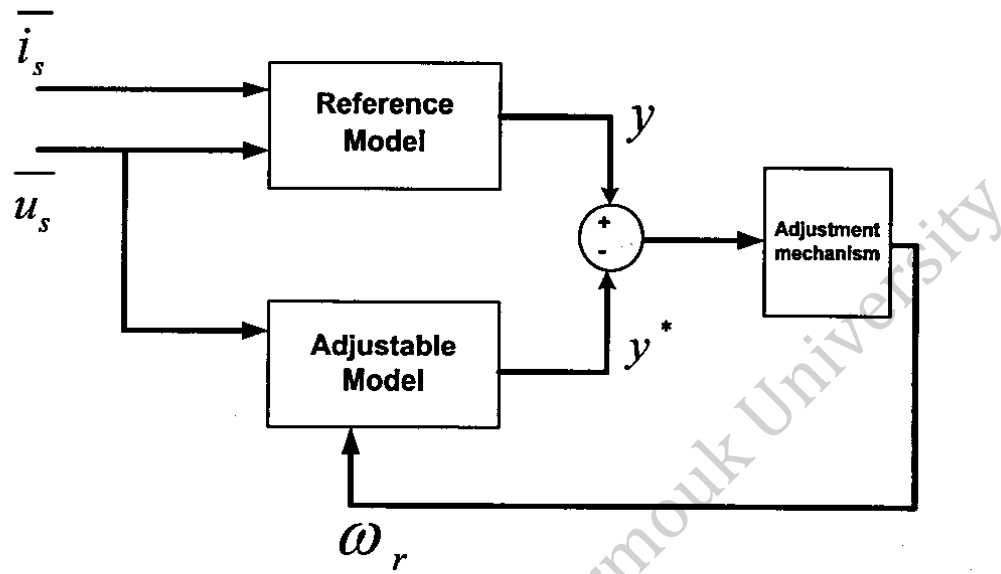
Figure 4.1: General MRAS scheme.

The MRAS control system can be given by using state equation as follows:

The reference model state equation is:

$$\frac{d}{dt} y = Ay + Bu$$

(4.1)

Where y is the state vector of the reference model; u is the input vector; A and B are constant matrices.

The adjustable model state equation is:

$$\frac{d}{dt} \hat{y} = \hat{A} \hat{y} + Bu$$

(4.2)

Where $\hat{y}$ is the estimated state vector of the adjustable model; u is the input vector; $\hat{A}$ and B are constant matrix.

Now defining the error vector e:

45

$$e = y - \hat{y}$$

(4.3)

The MRAS is designed now to minimize the error vector to zero in order to adjust the error in $A^\wedge$ which includes the estimated speed.

There are different choices for reference and adjustable model selection. The simplest model is choosing the reference model to be the stator currents which are measured from the motor and the adjustable model to be the current model of the motor itself.

To understand this choice of reference and adjustable model; the reference model output is the stator current vector i_s. It is simply done directly by measuring the stator current. Now the need for selecting an adjustable model that estimates the same state variable is obvious. The current model of the motor was chosen to be the reference model. Equations (2.5) and (2.6) are repeated here for convenience:

$$v_d = R_s i_d + L \frac{d}{dt} i_d - \omega_e L i_q$$

(2.5)

$$v_q = R_s i_q + L \frac{d}{dt} i_q + \omega_e L i_d + \omega_e \lambda_m$$

(2.6)

By arranging the above equations in term of stator currents, then:

$$\frac{d}{dt} i_d = -\frac{R_s}{L} i_d + \omega_e i_q + \frac{1}{L} v_d$$

(4.4)

$$\frac{d}{dt} i_q = -\frac{R_s}{L} i_q - \omega_e i_d - \frac{\lambda_m}{L} \omega_e + \frac{1}{L} v_q$$

(4.5)

46

Now in order to simplify (4.4) and (4.5); assume that [19, 23]:

$$
\begin{cases}
i_d = i_d^{'} - \dfrac{\lambda_m}{L} \\[2mm]
v_d = v_d^{'} - R\,\dfrac{\lambda_m}{L} \\[2mm]
v_q = v_q^{'} \\[2mm]
i_q = i_q^{'}
\end{cases}
\tag{4.6}
$$

Now substituting (4.6) into (4.4) and (4.5), then:

$$
\frac{d}{dt} i_d^{'} = -\frac{R_s}{L}\left(i_d^{'} - \frac{\lambda_m}{L} \right) + \omega_e i_q^{'} + \frac{1}{L}\left(v_d^{'} - R\,\frac{\lambda_m}{L} \right)
\tag{4.7}
$$

$$
\frac{d}{dt} i_q^{'} = -\frac{R_s}{L} i_q^{'} - \omega_e \left(i_d^{'} - \frac{\lambda_m}{L} \right) - \frac{\lambda_m}{L}\omega_e + \frac{1}{L} v_q^{'}
\tag{4.8}
$$

By arranging (4.7) and (4.8):

$$
\frac{d}{dt} i_d^{'} = -\frac{R_s}{L} i_d^{'} + \omega_e i_q^{'} + \frac{1}{L} v_d^{'}
\tag{4.9}
$$

$$
\frac{d}{dt} i_q^{'} = -\frac{R_s}{L} i_q^{'} - \omega_e i_d^{'} + \frac{1}{L} v_q^{'}
\tag{4.10}
$$

And in matrix form:

$$\frac{d}{dt}\begin{bmatrix} i\,_d \\ i\,_q \end{bmatrix} = \begin{pmatrix} -\dfrac{R_s}{L} & \omega \\ -\omega & -\dfrac{R_s}{L} \end{pmatrix}\begin{bmatrix} i\,_d \\ i\,_q \end{bmatrix} + \frac{1}{L}\begin{bmatrix} v\,_d \\ v\,_q \end{bmatrix}$$

(4.11)

Equation (4.11) is now similar to (4.1). It can be written as follow:

$$\frac{d}{dt}i\, = Ai\, + Bu\,$$

(4.12)

Equation (4.11) represents the reference model with i_s as a state vector. In practice, only a current sensor is required and this equation is only needed for the purpose of deriving the adaptation mechanism of the MRAS.

The adjustable model of the MRAS is chosen to be the current model of the motor. So the stator voltage will be the input vector of the adjustable model, and the estimated stator current vector will be compared with the measured one of the reference model. The error between the reference and adjustable model stator current will exist and it will be very high. This is because the adjustable model requires the motor speed information as shown in (4.13):

$$\frac{d}{dt}\begin{bmatrix} \hat{i}\,_d \\ \hat{i}\,_q \end{bmatrix} = \begin{pmatrix} -\dfrac{R_s}{L} & \hat{\omega} \\ -\hat{\omega} & -\dfrac{R_s}{L} \end{pmatrix}\begin{bmatrix} \hat{i}\,_d \\ \hat{i}\,_q \end{bmatrix} + \frac{1}{L}\begin{bmatrix} v\,_d \\ v\,_q \end{bmatrix}$$

(4.12)

$$\frac{d}{dt}\hat{i}\, = \hat{A}\hat{i}\, + Bu\,$$

(4.13)

48

Since the rotor speed information is not provided to (4.12) and (4.13), the error vector in (4.14) will be very high:

$$e = i^{'} - \hat{i^{'}}$$

(4.14)

If the error vector goes into an adaptation mechanism, which is a PI controller; then the error is minimized and the output of the PI controller will be the estimated rotor speed included in matrix A. This idea is shown in Figure 4.2.

Now the adaptive mechanism with the PI controller is given as follow [19]:

$$\begin{cases} \hat{\omega_e} = \left[K_p + \dfrac{K_i}{s} \right] \left[i_s \otimes \hat{i_s} \right] \\ \hat{\omega_e} = \left[K_p + \dfrac{K_i}{s} \right] \left[i^{'}_d \hat{i^{'}_q} - i^{'}_q \hat{i^{'}_d} \right] \end{cases}$$

(4.15)

Substitute (4.6) into (4.15); then:

$$\hat{\omega_e} = \left[K_p + \dfrac{K_i}{s} \right] \left[i_d \hat{i_q} - i_q \hat{i_d} - \dfrac{\lambda_m}{L} \left(i_q - \hat{i_q} \right) \right]$$
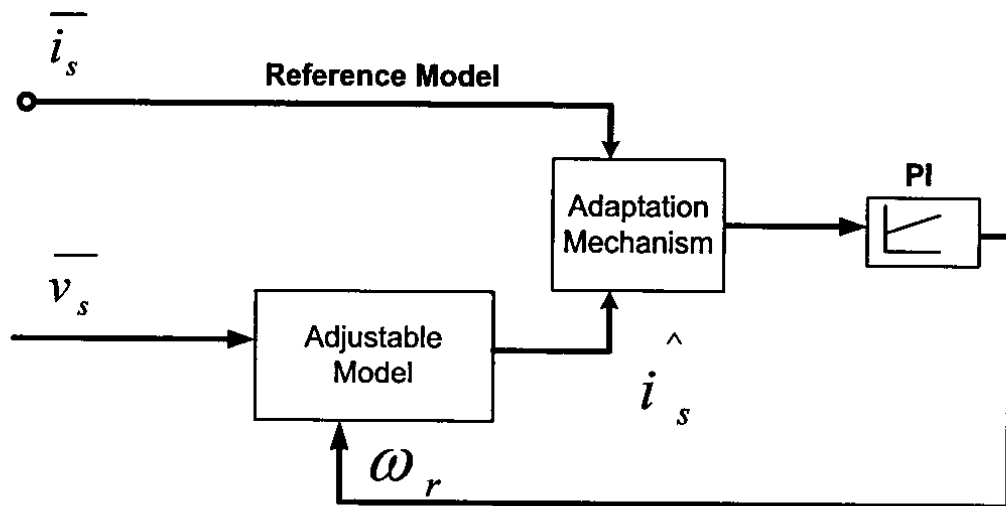
(4.16)

Figure 4.2: MRAS with motor current model.

Figure 4.3 shows the adjustable model of the MRAS modeled by MatLab/Simulink by using (4.12). It should be mentioned that the motor speed ω_e is the estimated value of the motor speed and it is provided by the adaptation mechanism as shown in Figure 4.2. Figure 4.4 shows the adaptation mechanism in MatLab/Simulink by using (4.16).

The final block diagram of the Speed Sensorless UPFC of SPMSM is shown in Figure 4.5.
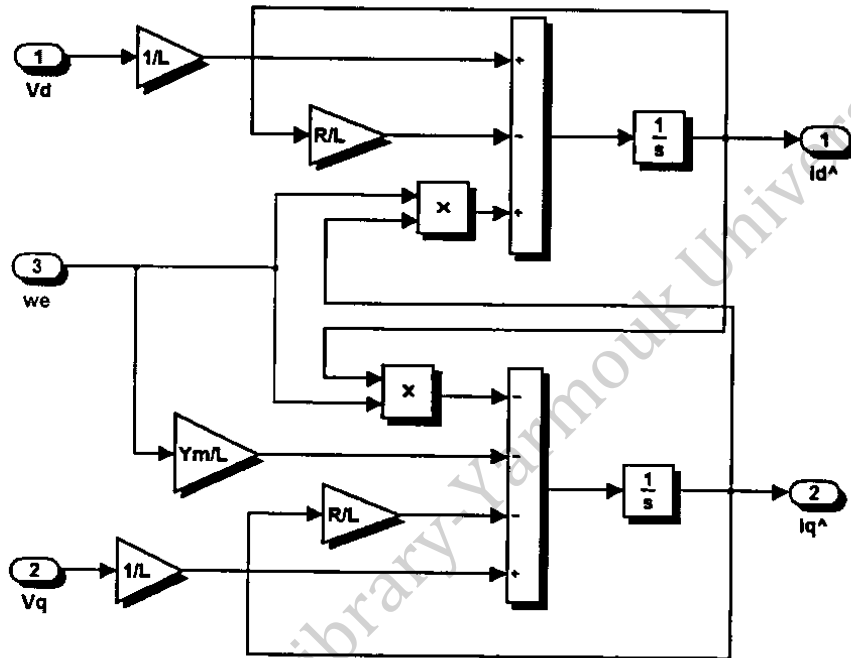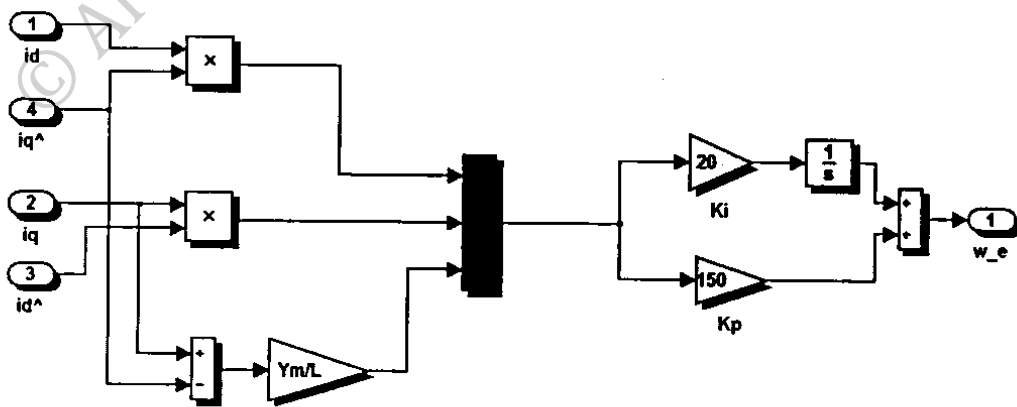
Figure 4.3: The adjustable model of the MRAS.

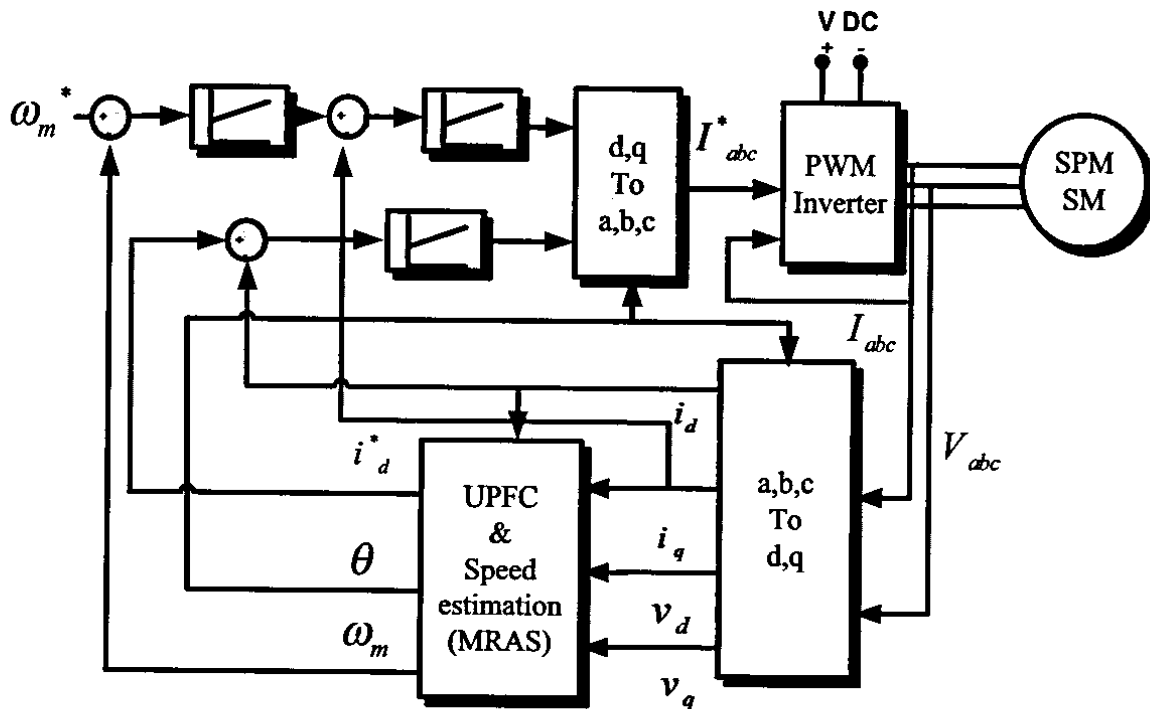Figure 4.4: The adaptive mechanism of the MRAS.

Figure 4.5: Block Diagram of Speed Sensorless UPFC of SPMSM.

4.3 Sliding Mode (SM) Model Reference Adaptive System

Adding the sign of the error signal between the estimated values of the stator currents and the actual measured stator current as feedback to the adjustable model of the MRAS, the sliding mode control is established as an error compensator to the error between the stator current vectors [20-26]. SMC generates high frequency discontinuous output that switches between 1 and -1. In [27], the authors stated that the MRAS for speed estimation based on the presented model used in this thesis doesn't ensure the convergence of the drive system. This has been showed in the simulation results. Adding the sliding mode concept has improved the response and convergence of the drive system.

52

The complete adjustable model equation using the sliding mode control is:

$$\frac{d}{dt}\hat{i}_d = -\frac{R_s}{L}\hat{i}_d + \omega_e\hat{i}_q + \frac{1}{L}v_d + D_s \qquad (4.16)$$

$$\frac{d}{dt}\hat{i}_q = -\frac{R_s}{L}\hat{i}_q - \omega_e\hat{i}_d + \frac{1}{L}v_q + D_s \qquad (4.17)$$

Where D_s is the sliding function such that:

$$D_s = k_s sign(\bar{i}_s - \hat{\bar{i}}_s) \qquad (4.18)$$

$$sign(\bar{i}_s - \hat{\bar{i}}_s) = \begin{cases} 1, & if\ \bar{i}_s > \hat{\bar{i}}_s \\ 0, & if\ \bar{i}_s = \hat{\bar{i}}_s \\ -1, & if\ \bar{i}_s < \hat{\bar{i}}_s \end{cases} \qquad (4.19)$$

The difference between the stator current and its estimate is used as a correcting signal in the adjustable model. The sliding mode gain k_s is adjusted so that the error is converged to zero as fast as possible, i.e. the error between the estimated and the actual stator current approaches zero so that the sliding surface is achieved [22, 25]. This yields an accurate estimation of the motor speed and the error between the actual and estimated speed approaches zero. The value of k_s is tuned in simulation (using trial and error method) such

that the error is decreased and the transient behavior is improved. The block diagram of the MRAS with the Sliding Mode concept is shown in Fig 4.6.
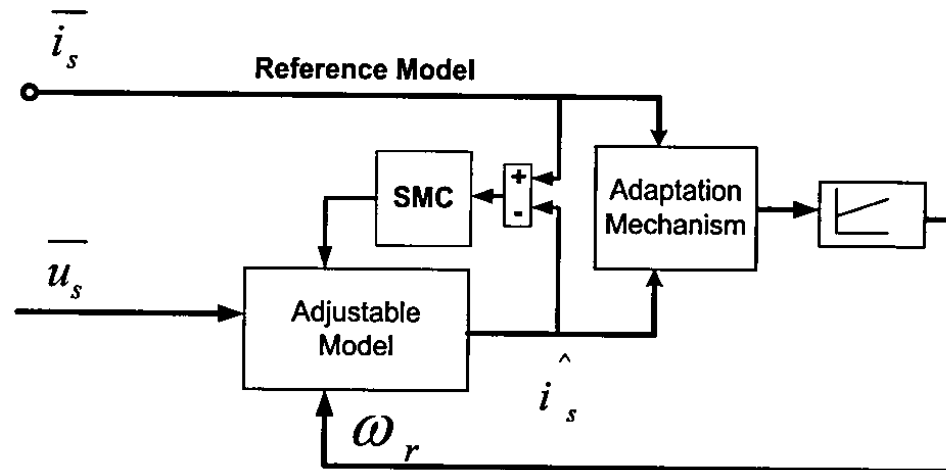
Figure 4.6: MRAS with SM concept.

A problem appeared in the MRAS with the SMC; the sliding mode gain is adjusted and the error between the actual and reference rotor speed was reduced. But when the reference speed or the motor load torque was changed; this error has increased but the system stayed stable. The sliding mode gain has to be modified when the motor load or speed is changed. In order to solve this problem and reduce the error and keep it close to zero; a PI controller in Figure 4.2 is replaced with a FLC as shown in Figure 4.7.

54

Figure 4.7: MRAS with Fuzzy Logic Controller.
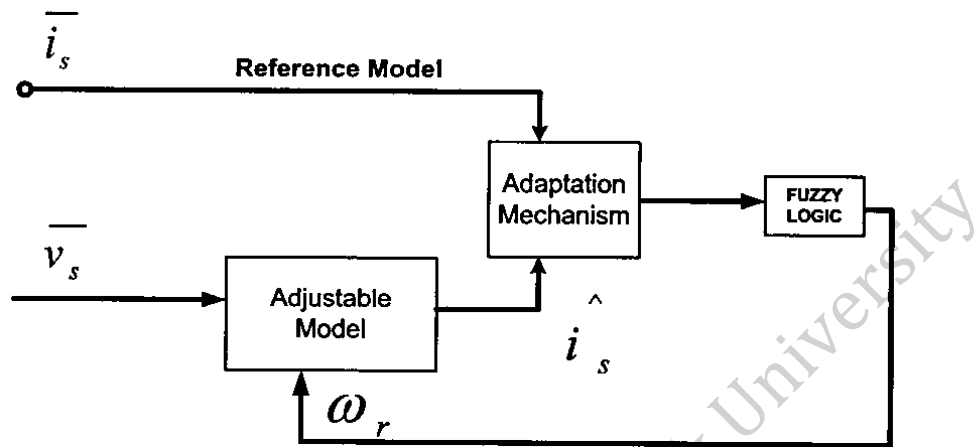
4.4 Fuzzy Logic Control

Fuzzy set theory is first proposed by Prof. L. Zadeh in 1965. It is developed by comparing the concepts and operations of fuzzy sets with those of classical set theory. FLC has been used in a variety of control systems and become the best alternative for nonlinear controllers by using of heuristic information. FLC is superior to traditional PI controllers since it can cover a wider range of operating conditions and adapts its output to fit the demand control performance. FLC can be imagined as a PI controller with a human as an operator who will tune the PI controller to get the desired performance when the operating condition is changing frequently.

The next subsections will review the basic concepts of the fuzzy logic theory and the elements of the FLC.

4.4.1 Universe of Discourse

The universe of discourse is simply any ordinary input or output sets. In real world; the universe of discourse represents real numbers, intervals or subset of real numbers.

4.4.2 Linguistic Variables

Linguistic variables are constant symbolic descriptions of any time-varying quantity. Linguistic variables describe the inputs and outputs of any fuzzy system. Examples of linguistic variables are the temperature, speed, age, weight ... etc.

4.4.3 Linguistic Values

Linguistic values can be described simply as how a human will define the linguistic variables. In the case of 'Temperature' as a linguistic variable, the linguistic values that will clearly define the temperature will be: Low, High, Very Low, and Very High. In the case of "the age" as another example of linguistic variable, the linguistic values will be: old, very old, young and very young.

4.4.4 Fuzzy Membership Function

The membership function for fuzzy sets is a function which relates the linguistic variables with numbers at the universe of discourse. Different shapes of Membership

functions can be used as shown in Figure 4.8. The most common used membership function is the triangular function.
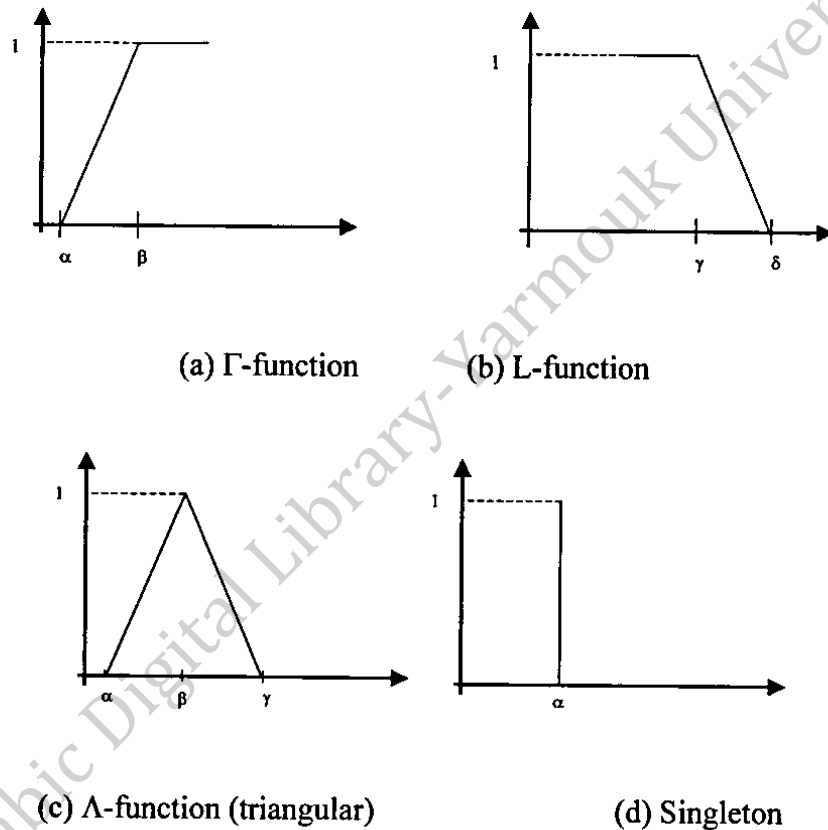

(a) Γ-function   (b) L-function

(c) Λ-function (triangular)   (d) Singleton

Figure 4.8: Membership Functions examples.

4.4.5   Fuzzy Sets

Let U be a collection of numbers which represents the universe of discourse; the characteristic function (called membership function) of a fuzzy set A is expressed as follow:

$$\mu_A : U \rightarrow [0,1] \tag{4.20}$$

Where μ_A represents the membership function and gives the degree of membership for each element of the universe of discourse which can take any value between 0 and 1. The

57

value of μ_A is called the degree of membership. For example, the membership function of a TEMPERATURE μ_T is considered; then the temperature can be described as VERY COLD, COLD, HOT and VERY HOT. Considering only the HOT temperature for simplicity; one can express that 27°C is hot but not as hot as 30 °C. And 25 °C and bellow is completely not hot. Figure 4.9 shows the membership function μ_T for the fuzzy set Temperature T.

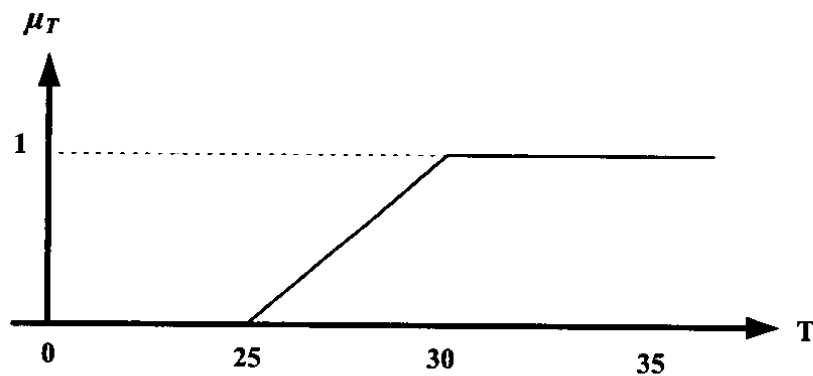Figure 4.9: The Membership Function μT.

4.4.6 Fuzzy Set Operations

The logical operations, union, intersection, and complement, can be applied to any fuzzy sets as in the crisp sets. The membership function of the union of two fuzzy sets A and B with the membership functions $\mu_A(x)$ and $\mu_B(x)$ has a new fuzzy set C. where $C=A \cup B$ and:

$$\mu_C(x) = max\{\mu_A(x), \mu_B(x)\} \tag{4.23}$$

Figure 4.10: Union of Two Fuzzy Sets.

The membership function of the intersection of two fuzzy sets A and B with the membership functions $\mu_A(x)$ and $\mu_B(x)$ has a new fuzzy set C, where $C=A\cap B$ and:
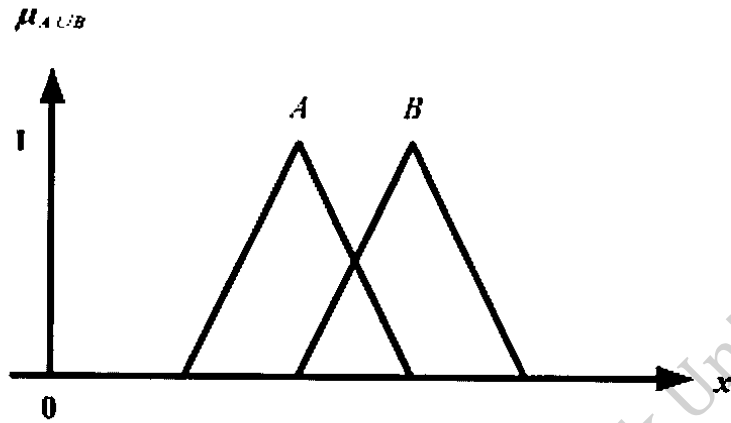
$$\mu_C(x) = min\{\mu_A(x), \mu_B(x)\} \tag{4.24}$$
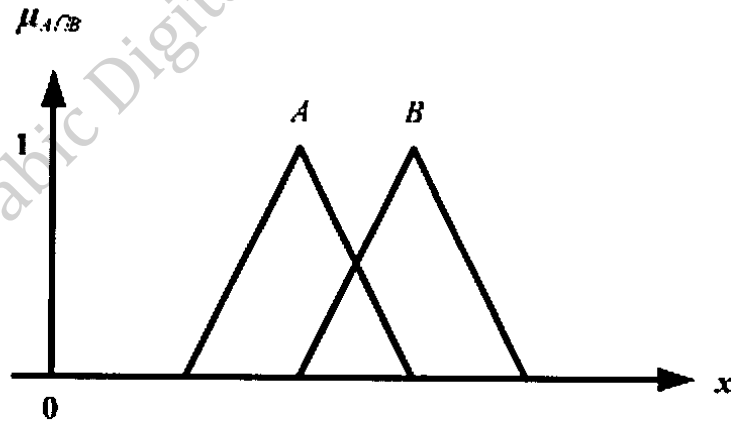
Figure 4.11: Intersection of Two Fuzzy Sets.

The membership function of the *complement* of a fuzzy set A $(A^{\backslash})$, is:

$$\mu_A^{\backslash}(x) = 1- \mu_A(x) \tag{4.25}$$

Figure 4.12: Complement of a Fuzzy Set.

4.4.7 Fuzzy Control System

There are five principal components of the FLC as shown in Figure 4.13, they are [1]:

- Fuzzification module (fuzzifier).

- Knowledge base.

- Rule base.

- Inference engine.

- Defuzzification module (defuzzifier).

A brief description of each component is listed below.

Figure 4.13: Block diagram of a typical fuzzy logic controller.

4.4.7.1 Fuzzifier

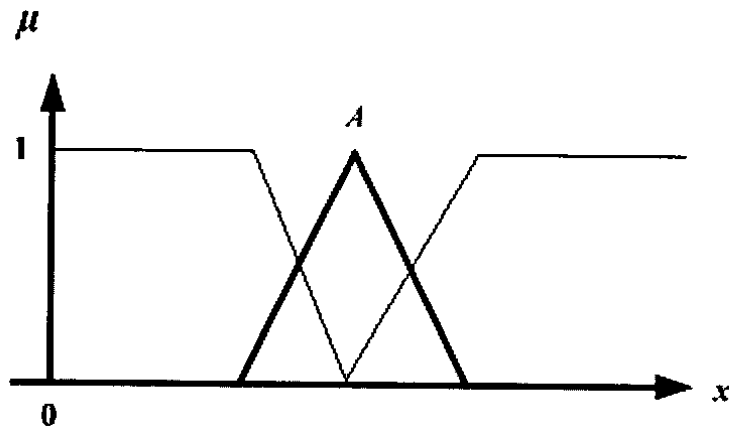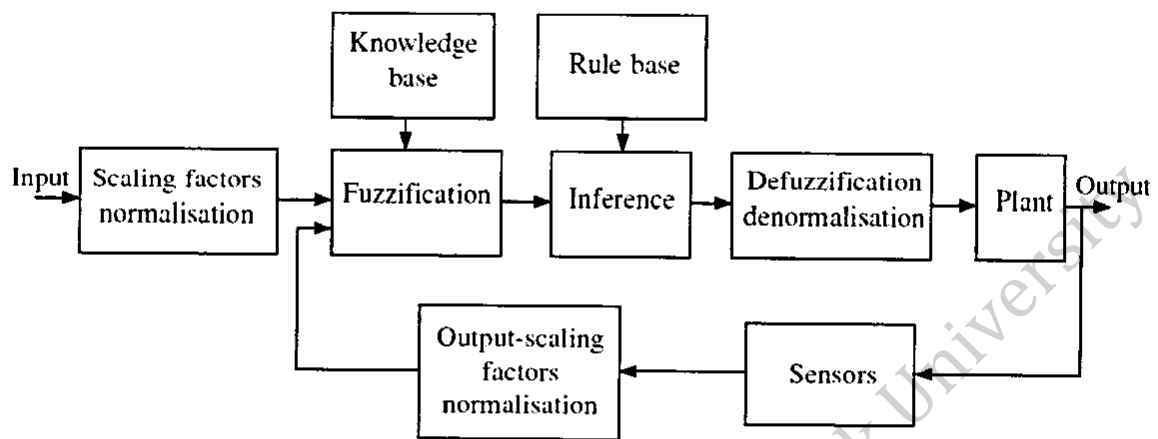The fuzzification module converts the inputs from a crisp values into fuzzy values, so that they are readable with the fuzzy set representation in the rule base.

4.4.7.2 Knowledge Base

The knowledge base consists of a database of the plant. It provides all the necessary definitions for the fuzzification process such as membership functions, fuzzy set representation of the input–output variables and the mapping functions.

4.4.7.3 Rule Base

The rule base is the control strategy of the system. It is expressed as a set of IF-THEN rules. The rules are based on the fuzzy inference concept and the antecedents and consequents are associated with linguistic variables. The rules are interpreted using a fuzzy inference technique. In fuzzy control theory, this is normally Mamdani's inference technique [1].

61

4.4.7.4 Defuzzifier

Defuzzifier converts the fuzzy sets generated by fuzzy inference in fuzzy rules into a real number as the output of the FLC.

Chapter 5 SIMULATION RESULTS

In this chapter, simulation results of the new control system using Matlab/Simulink software are presented. The validity and accuracy of the used controller has been verified.

5.1 Steady state performance curves.

The steady state equations presented in chapter 3 are used here to study the performance of the SPMSM with UPFC. A comparison between the UPFC and MTPAC is presented here. The only difference in the equations is the value of i_d is equals to zero in MTPAC. The motor parameters are presented in chapter 2 and it is repeated here for convenience. The m-file which computes and plots the performance curves is located in Appendix A.

Table 2.1: SPMSM Parameters

The stator resistance Rs (Ω)	1.4
The stator inductance L (H)	0.0066
The PM flux λ_m (web)	0.1546
Number of Poles P	6
J (kg.m^2)	0.00176
B (N.m.s)	0.00038818
T_n (N.m)	7
f (Hz)	50

Initially; assume that the motor is loaded with nominal torque of 7 N.m, and the command speed of the motor is increased. It is clear that the stator current will remain constant since it depends only on the motor torque. This is shown in Figure 5.1. The solid line represents the stator current amplitude (Peak to Peak) of the UPFC and the dashed one represents amplitude of the stator current of the MTPAC. It is clear that the stator current of the MTPAC is less than the UPFC since the value of i_d is kept to zero. This will reduce the current losses and the motor under UPFC will consume more current than that of the MTPAC. The powerful of the UPFC will be shown in the next figure by calculating the required stator voltages of the SPMSM under different rotor speed.
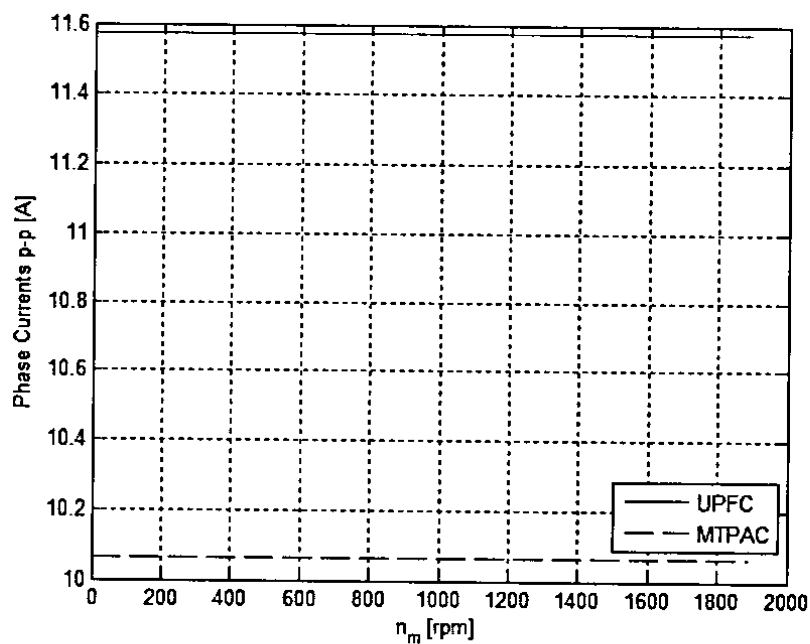

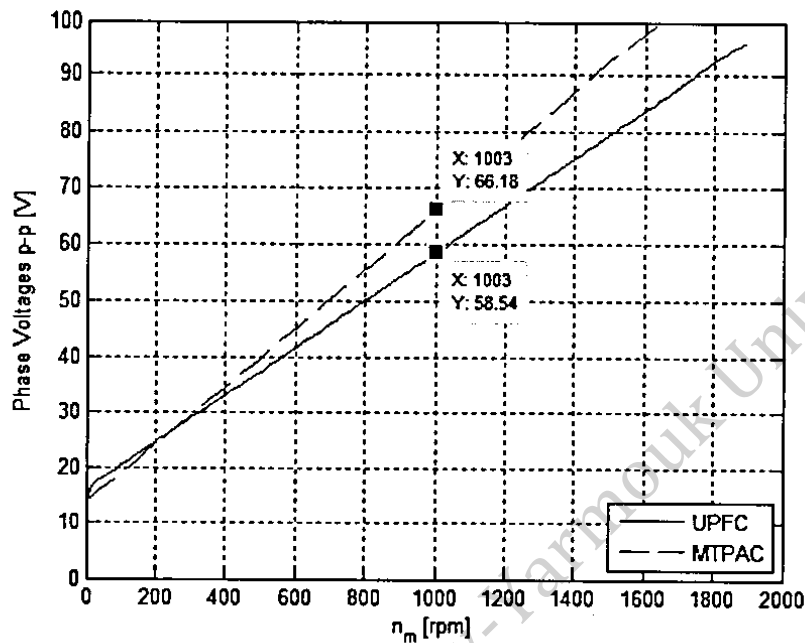Figure 5.1: Stator current under different speeds and at 7 N.m.

Figure 5.2: Stator voltage under different rotor speeds and at 7 N.m.

Figure 5.2 shows the required values of the stator voltage under different speed commands and at 7 N.m load. It is clear that the stator voltage under UPFC is less than that of MTPAC. Taking into consideration the nominal rotor speed which is 1000 rpm in Figure 5.2, the peak value of the stator voltage under MTPAC is 66 volt. While under UPFC it is 58 volt. This means that if the assumption was made about the maximum peak value of the VSI output voltage to be 66 volt; then the UPFC will drive the motor at its nominal speed and the supply voltage will be 58 volt, and the extension of operating the motor above the base speed until reaching the value of 66 volt of the VSI output voltage is possible. The rotor speed under UPFC and 66 volt is shown in Figure 5.2 to be 1180 rpm. This explains the idea of extending the constant torque region above the rotor's base speed by using UPFC of SPMSM. This idea is shown in Figure 5.3.

65

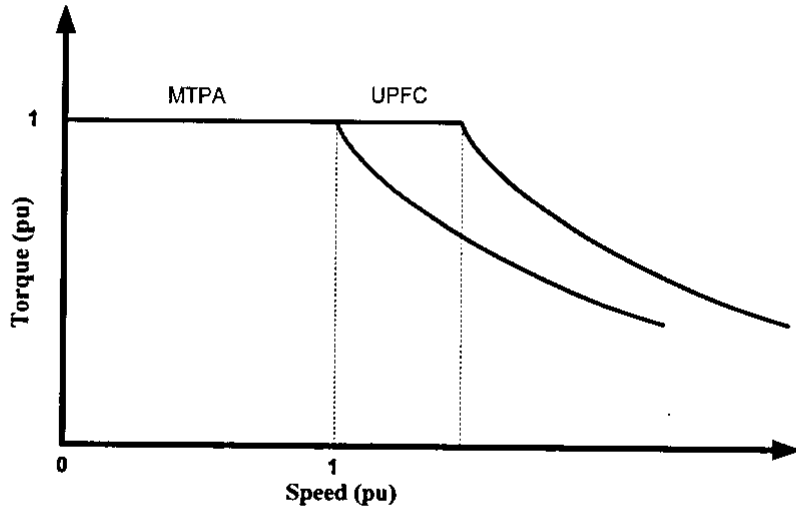Figure 5.3: The constant torque region under MTPAC and UPFC.

Now assume that the motor is running at constant speed of 1000 rpm. By increasing the motor load; the stator current will also increase but the stator current of the UPFC will be higher than that of MTPAC. Figure 5.4 shows the peak value of the stator current running under UPFC and MTPAC.
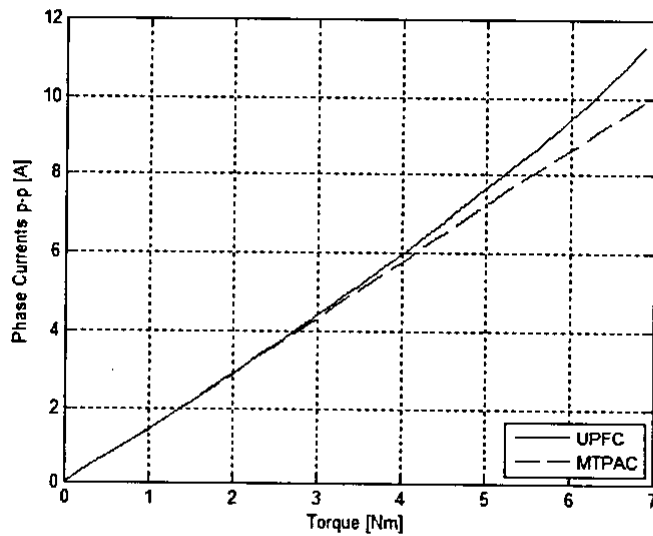

Figure 5.4: Stator current vs. Torque at 1000 rpm.

66

5.2 UPFC of SPMSM.

UPF controller model is shown in Figure 5.5. The system gets the rotor speed from the motor model; i.e. using a mechanical sensor for measuring the speed and the rotor position. The sensorless UPFC is shown in the next section.

Figure 5.5: Simulink model of Unity Power Factor Control of SPMSM

The VSI is modeled based on sinusoidal PWM technique. The DC bus voltage is 200 volt and the frequency of the reference triangle signal is 4K Hz. A low pass filter is used to smooth the output voltage of the VSI since a simulation model of the motor is used as shown in Figure 5.6. The motor is loaded with 7 N.m load torque and a step speed command of 1000 rpm is applied to the controller. The UPF calculator used to calculate the reference i_d current is modeled based on equation (3.17).

Figure 5.7 shows the speed step response of the SPMSM. The PI controller coefficients were set by trial and error.
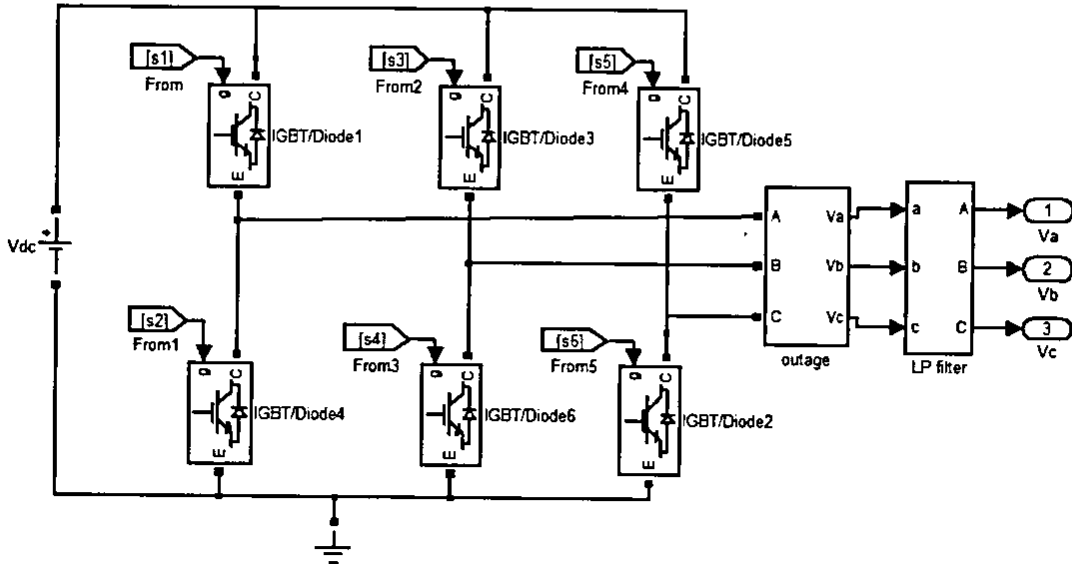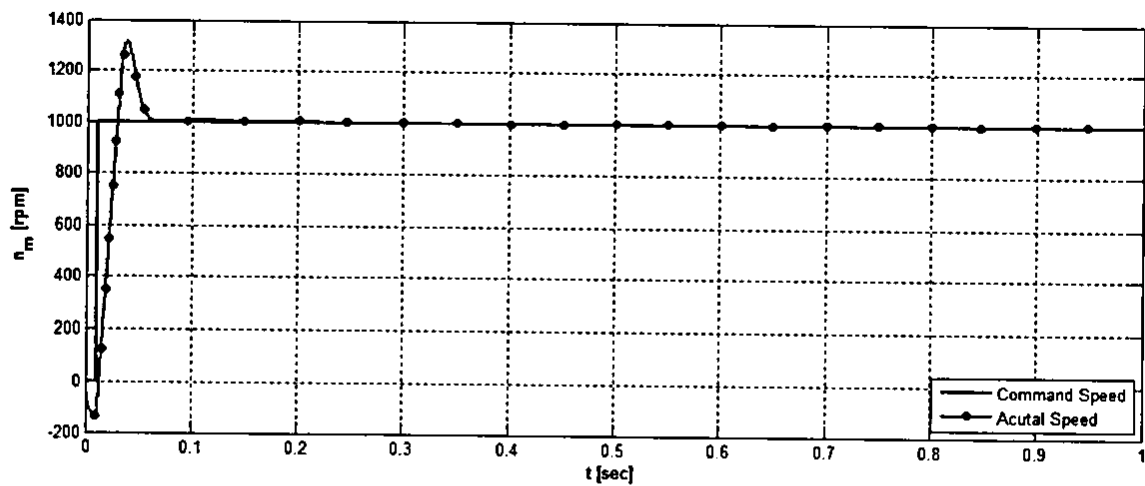

Figure 5.6: Simulink model of VSI

Figure 5.7: Speed step response at 7 N.m using a speed sensor.

68

Figure 5.8 shows the three phase stator current of the motor where its amplitude matches the value presented in Figure 5.4 at 7 N.m.
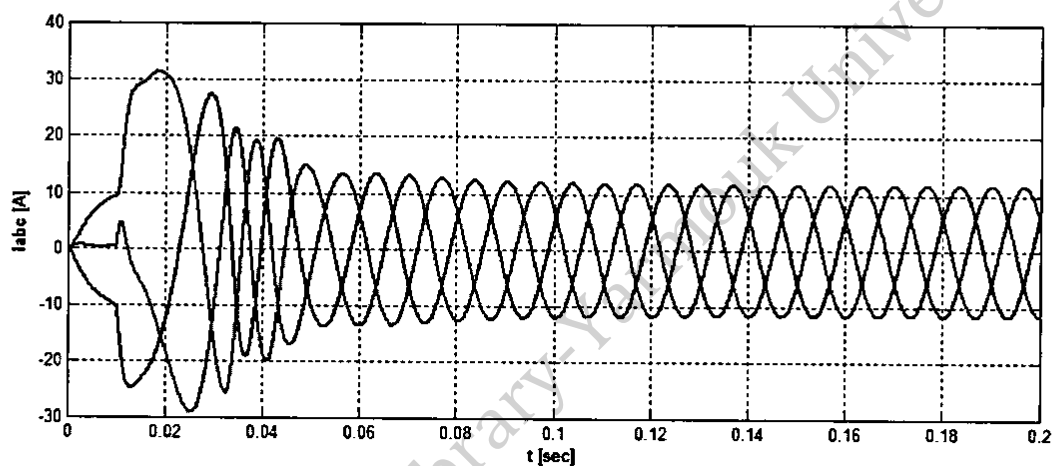

Figure 5.8: Instantaneous three-phase currents at 7 N.m & 1000 rpm.
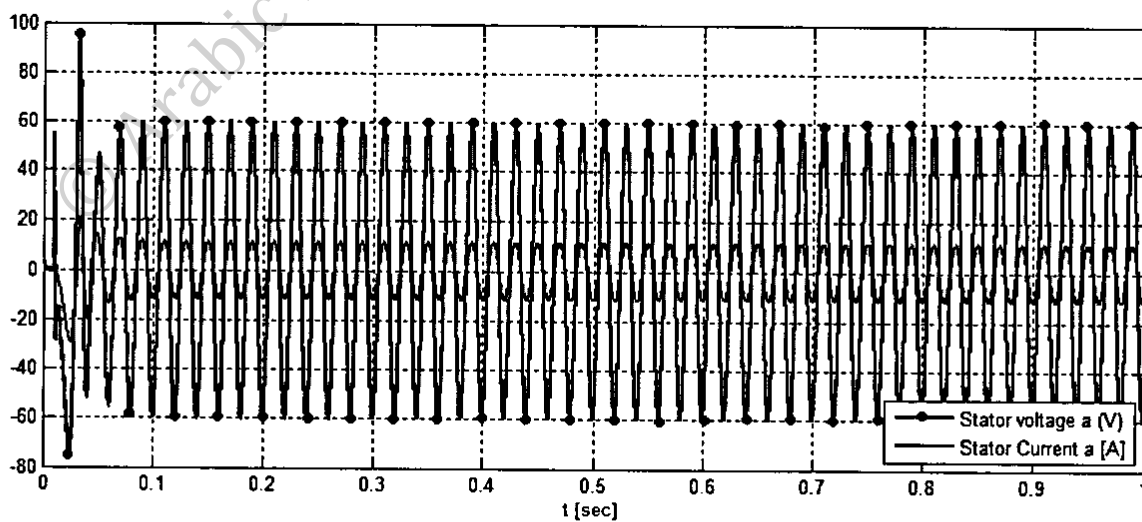

Figure 5.9: Instantaneous stator Voltage and Current of phase a.
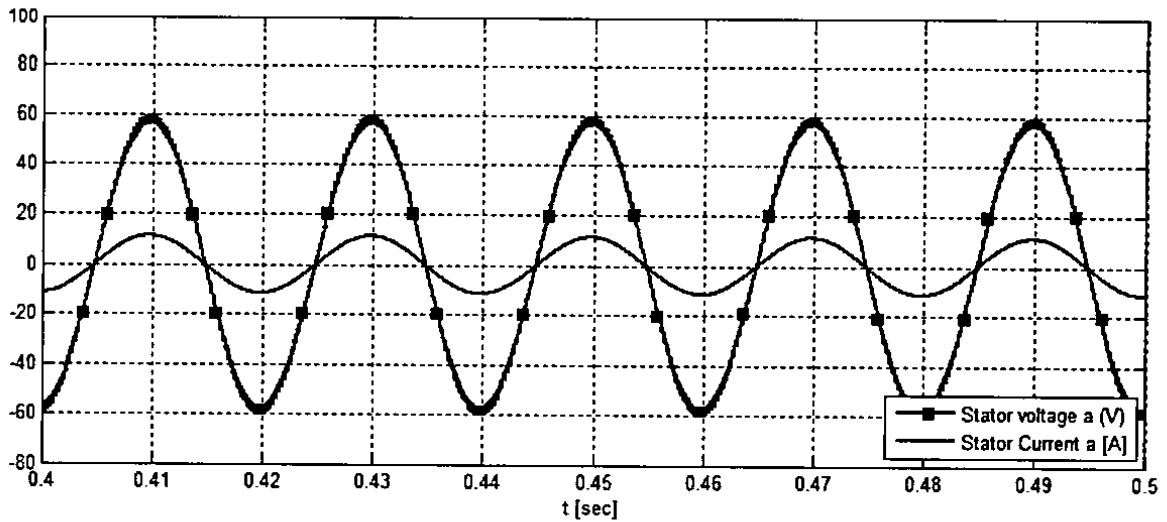
Figure 5.10: Zoomed Stator Voltage and Current of phase a.

In Figure 5.9; phase a stator current and voltage are plotted together. A zoomed figure as in Figure 5.10 shows that the stator current and voltage are in phase and the power factor here equals one. This means that there is no phase difference between the stator voltage and current. As mentioned previously, this will reduce the required VA rating of the VSI and extend the constant torque region of the motor.

Figure 5.11: The response of the developed Torque of the SPMSM at 7 N.m Load.

Figure 5.11 shows the response of the developed torque of the motor. It is clear that the motor is required to develop high torque when star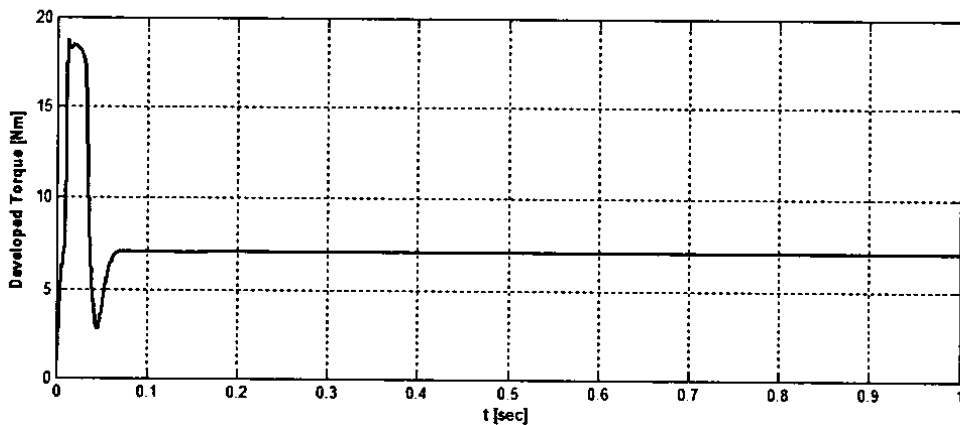ting in order to drive the load at the desired speed. The developed torque is then goes into steady state and approaches the load torque.

A new command speed is now applied to the motor with the same previous load torque value. At the beginning, the speed command equals the motor base speed, and then it goes down to zero. Another command of 500 rpm is then applied. The response of the motor speed is shown in Figure 5.12.

It is clear from Figure 5.13 that the motor speed directly depends on the stator current and voltage frequency. When the motor speed command was reduced to 500 rpm, the frequency of the stator voltage decreased too. The developed torque response is shown in Figure 5.14.
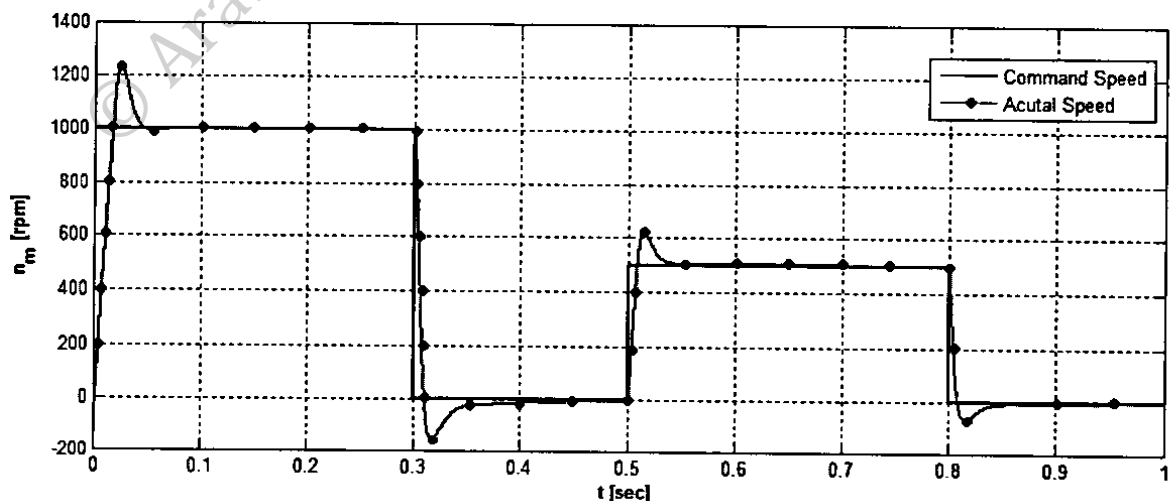
Figure 5.12: Speed step response at different command speed using a speed sensor.
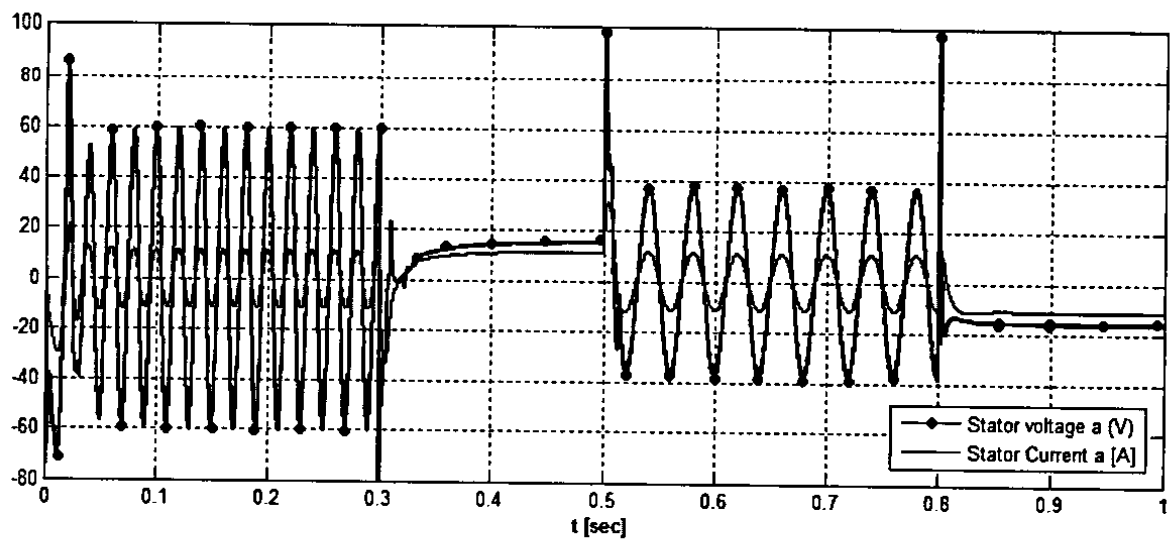
Figure 5.13: Instantaneous stator current and voltage at different command speed.
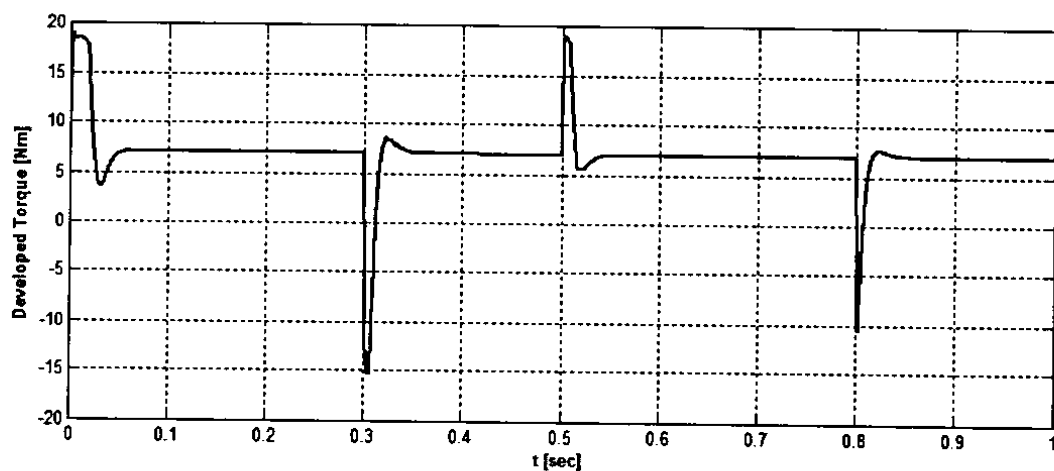
Figure 5.14: Developed Torque response at different command speed.

5.3 MRAS Speed Sensorless Control UPFC of SPMSM.

The simulink model of the MRAS for speed estimation of SPMSM is shown in Figure 5.15. The system was shown in Figure 4.3 and 4.4. The command speed is 1000 rpm and the load torque is 7 N.m. The simulation result of the speed response is shown in Figure 5.16.
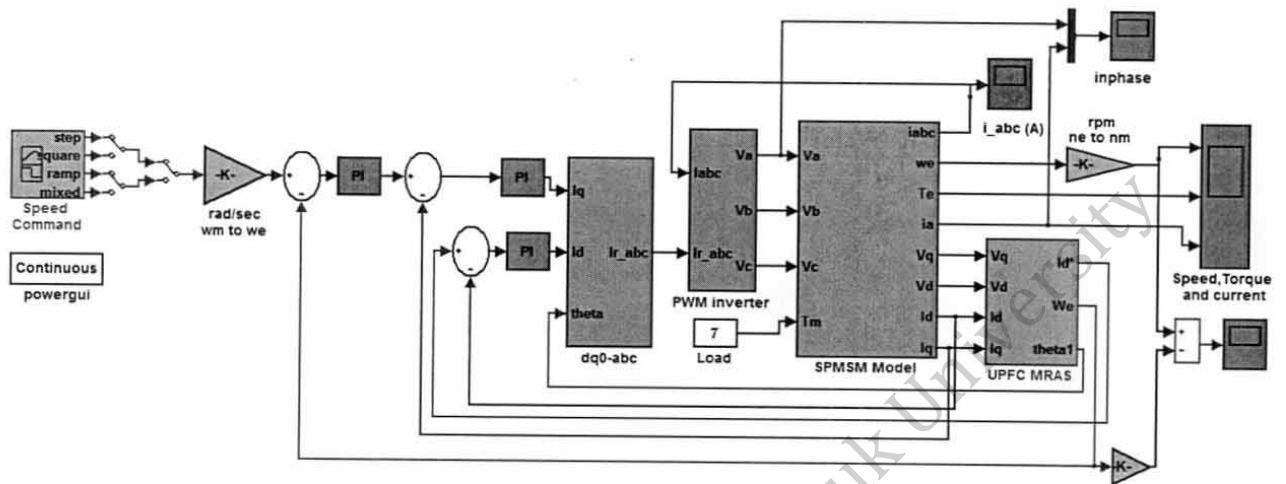
Figure 5.15: Simulink model of Speed Sensorless MRAS based, and UPFC of SPMSM
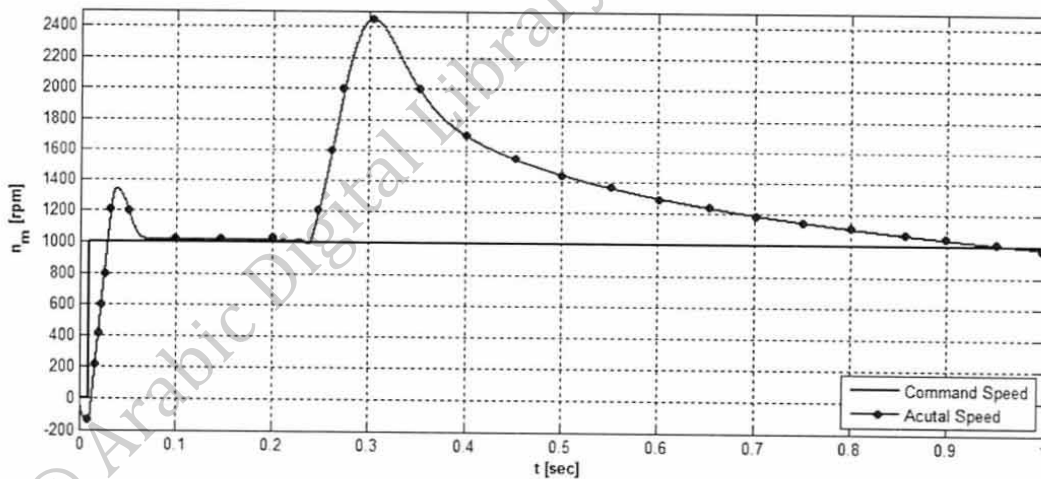
Figure 5.16: Speed response of sensorless MRAS based system.

In Figure 5.16, the adaptation process in rotor speed estimation was good before the time of 0.2 sec. After 0.2 sec the speed of the motor doesn't converge to the desired speed as well as the estimated speed of the motor. Incorporating the sliding mode idea to the MRAS by taking the sign of the difference between the measured stator current (the

reference model) and the estimated stator current (the adaptive model) and feedback them to the reference model will insure the convergence of the rotor speed. This is clear in Figure 5.17. The sliding mode coefficient is set to 40.
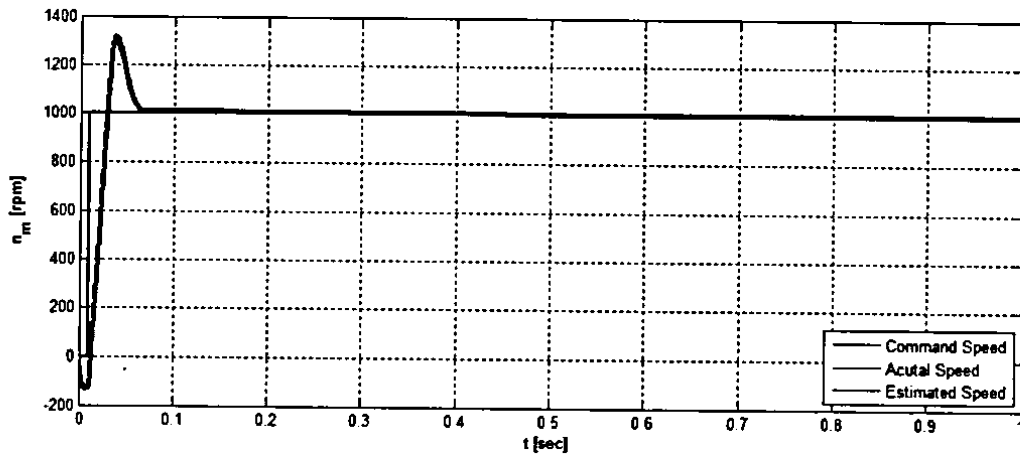
Figure 5.17: Speed response of sensorless SM MRAS based system and UPFC.

The error between the actual rotor speed and the estimated speed is close to zero, this is shown in Figure 5.18.
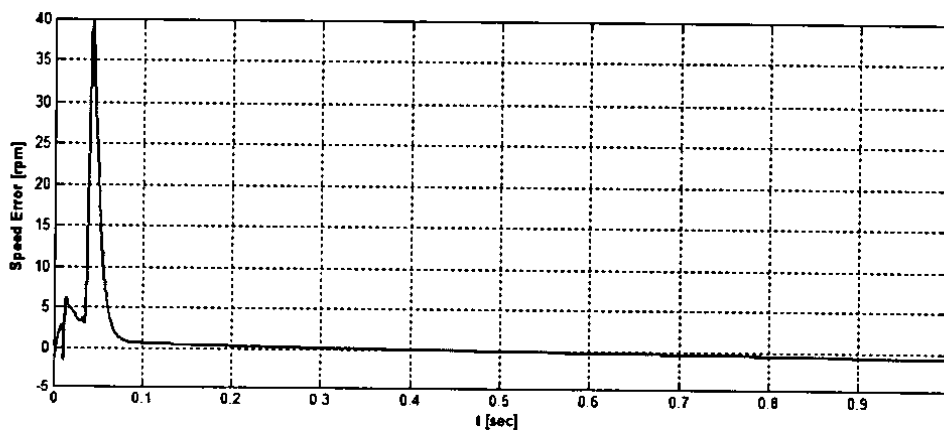
Figure 5.18: Error between the actual and estimated rotor speed under SM MRAS and UPFC.

74

It is also important to check for the unity power factor operation under Sliding Mode MRAS. Figure 5.19 shows that the stator current and voltage are in phase, so the power factor equals one. Figure 5.20 shows the developed torque response.
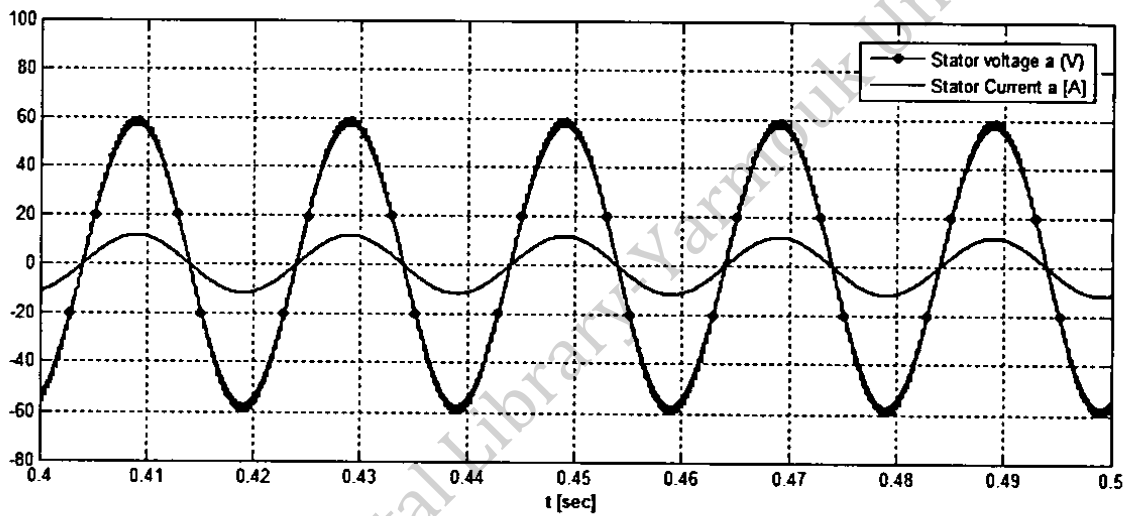
Figure 5.19: Stator current and Voltage under SM MRAS and UPFC.
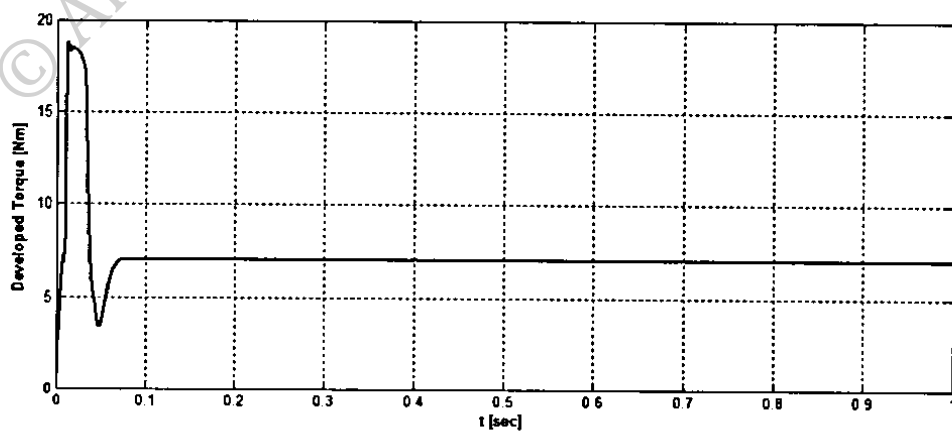
Figure 5.20: Developed torque response under SM MRAS and UPFC.

The problem in this model is that if the load torque is changed or the reference speed of the motor is changed; the error between the actual and estimated speed will increase. The sliding mode coefficient should be changed in order to minimize the error. This problem triggers the idea of using a FLC instead of a PI controller. To demonstrate this problem, the load torque has been changed to 3 N.m without changing the command speed, Figures 5.21 and 5.22 show how the error between the actual and estimated rotor speed became greater than zero.
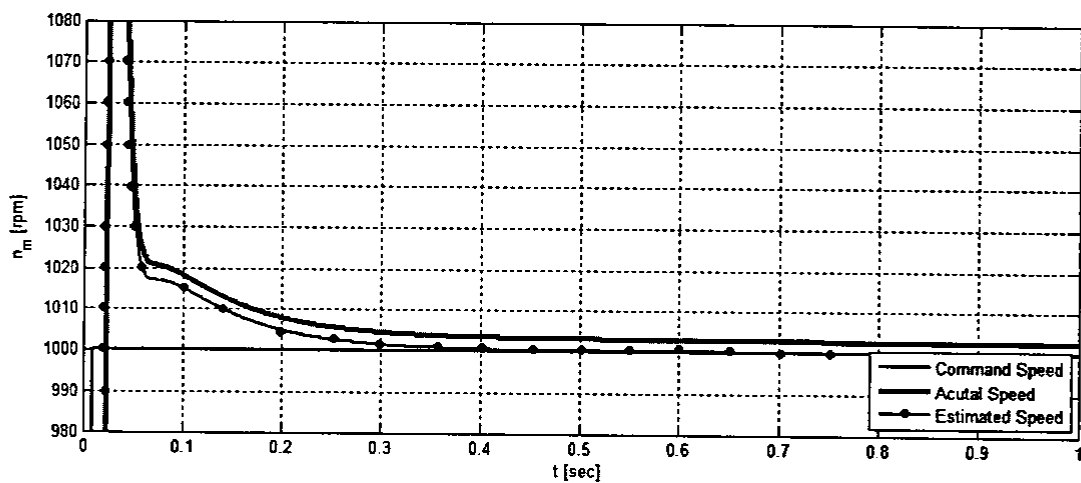
Figure 5.21: Speed response under SM MRAS and UPFC when the load torque is changed.
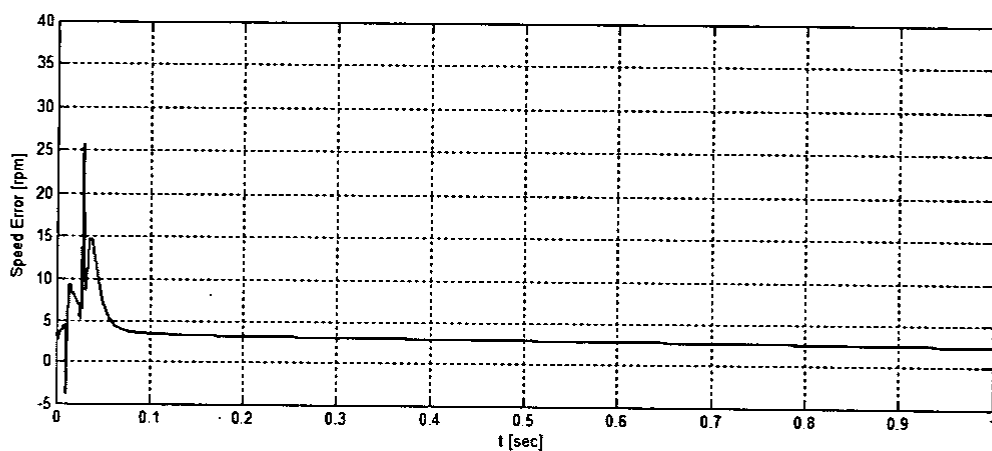
Figure 5.22: Error between the actual and estimated rotor speed when the load torque is changed.

5.4 Speed Sensorless MRAS with FLC and UPFC of SPMSM.

The Simulink model of the MRAS with FLC is shown in Figure 5.23. FLC is modeled using the MatLab Fuzzy Logic toolbox GUI. The advantage of using FLC is clear as shown in the simulation results which show that the error between the actual and estimated rotor speed is minimized to zero regardless of changes made on the motor load torque or reference speed.
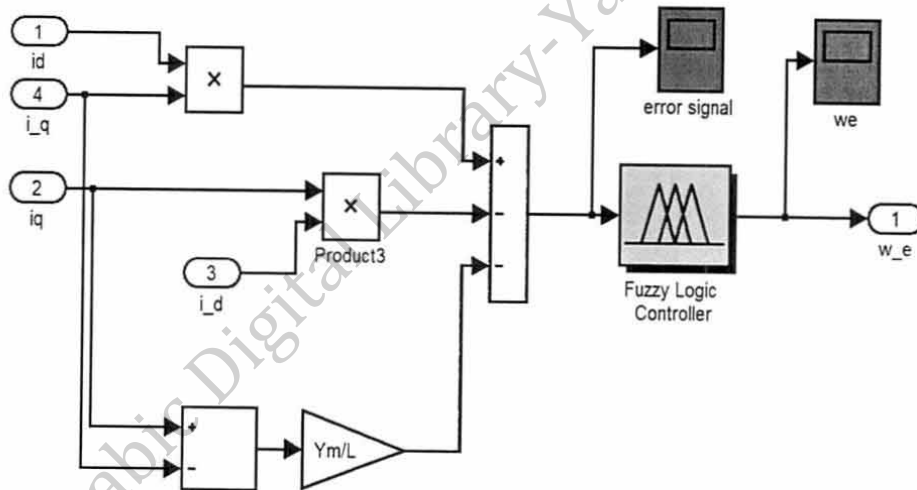
Figure 5.23: MRAS with Fuzzy Logic Controller

The control task that should be performed by the FLC is to reduce the error signal to zero such that the estimated rotor speed is very close to the actual rotor speed. The estimated speed in Figure 5.23 is the electrical angular speed, and it should be considered in tuning the FLC. It should be mentioned that tuning the FLC is iterative; several combinations of membership functions has been tested.

Now the input set point should be defined in order to tune the FLC. As the input to the FLC is the error signal, then the set point is Zero. If the error signal goes high above the set point; then the output estimated speed should be increased. And if the error signal goes low below the set point; then the output estimated speed should be reduced. Finally, if the error signal is about the set point; then the output estimated speed shouldn't change much.

Now let the input status words to be: Negative (N), Zero (Z), and Positive (P).

And let the output action words to be: More speed (GP), No change (Z), and Less speed (GN).

Now the rule-base is as follow:

1. **If** the error signal is high (P), **then** more speed (GP).

2. **If** the error signal is about zero (Z), **then** no change (Z).

3. **If** the error signal is low (N), **then** less speed (GN).

The membership functions for both the input and the output of the FLC are shown in Figures 5.24 to 5.26.
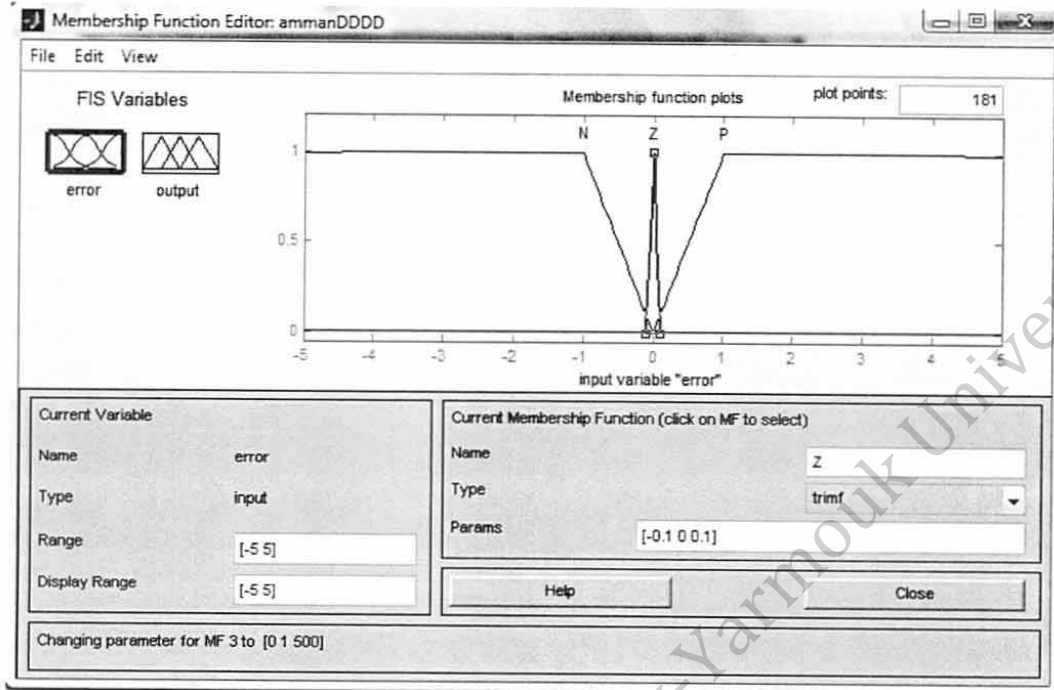
Figure 5.24: Input membership function
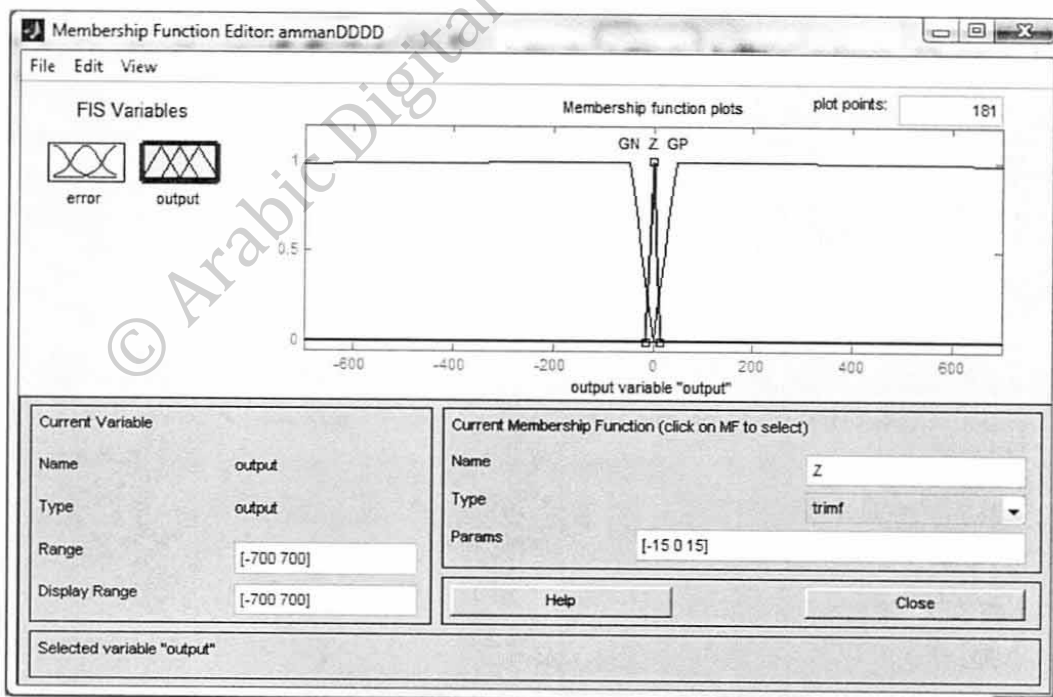
Figure 5.25: Output membership function
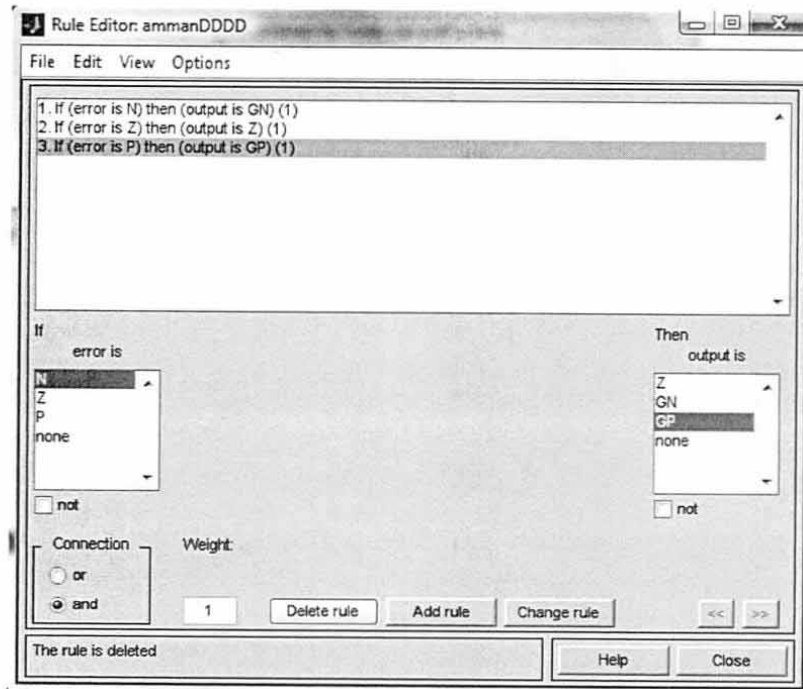
Figure 5.26: Rule Base

It is clear that the modeled FLC is very simple but a problem occurs regarding the estimated speed; the estimated speed will fluctuate at high frequency. So another input to the FLC should be added which is the rate of change of the error signal so that the estimated speed will change its value smoothly. However; and for more simplification of the control system; only one input membership function is applied and a Low Pass Filter (LPF) is used to smooth the estimated speed which used in the adaptive model and the PI speed controller. Figure 5.27 shows the idea of adding the LPF instead of adding a new input membership function for the rate of change of the error signal.

From the Motor

$$(-Ym+sqrt(Ym^2-4*L^2*u[1]^2))/(2*L)$$

equation (3.17)

butter

4
Iq

1
Id*

Id_Ref

From the Motor

FLC MRAS

2
Vd

ud

1
Vq

uq

theta

3
theta

3
Id

id

iq

w_e

butter

rpm

-K-

estimated speed

LPF

2
We
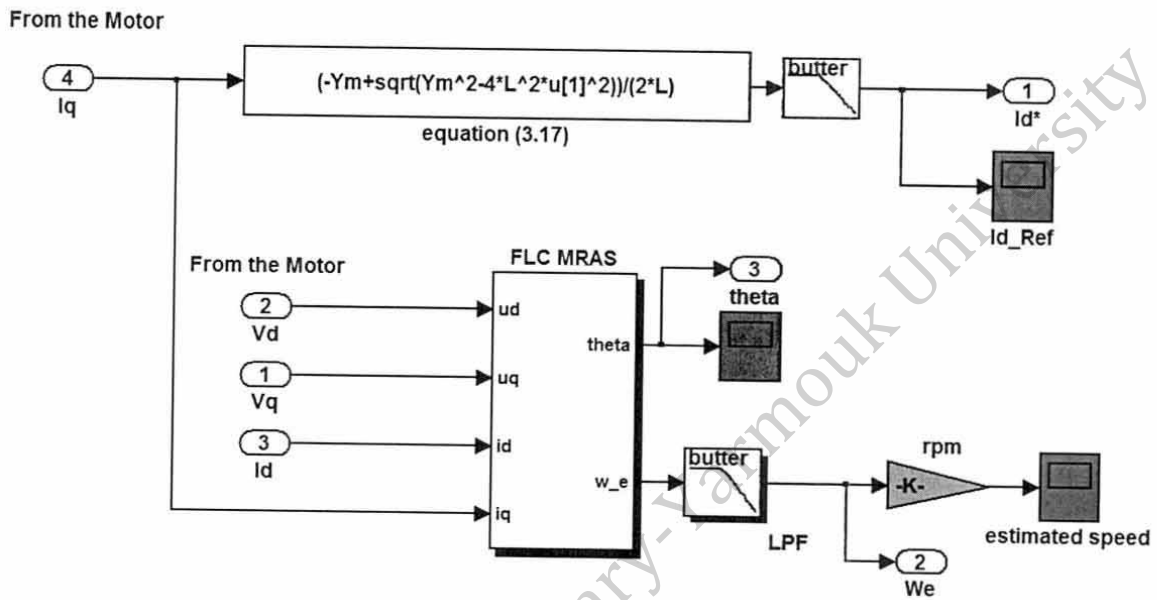
Figure 5.27: Simulink model of the FLC MRAS with LPF of the estimated speed

Figures 5.28 to 5.30 show the simulation results of the speed sensorless MRAS with FLC and UPFC. The command speed is 1000 rpm and the motor load torque is 7 N.m. The results shows that the unity power factor operation is achieved under this control approach, moreover the accuracy of the estimated rotor speed is very high and much better than that of MRAS SM based system.

stator voltage (V) ▬■▬
stator current (A) ────

Time (sec)
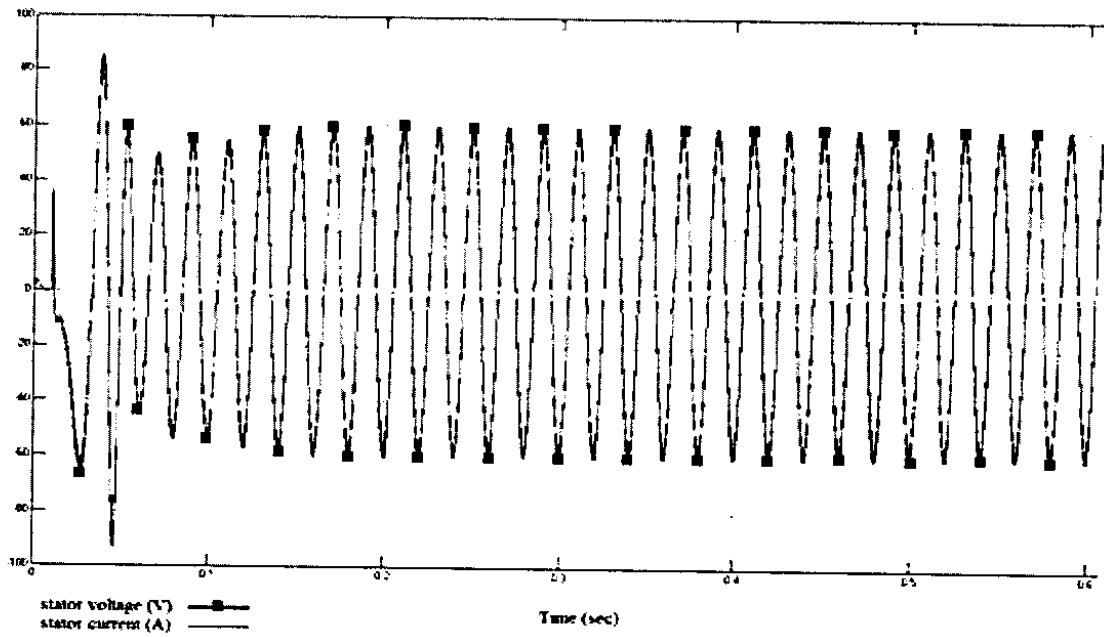
Figure 5.28: Instantaneous stator current and Voltage at 7 N.m and 1000 rpm

Time (sec)
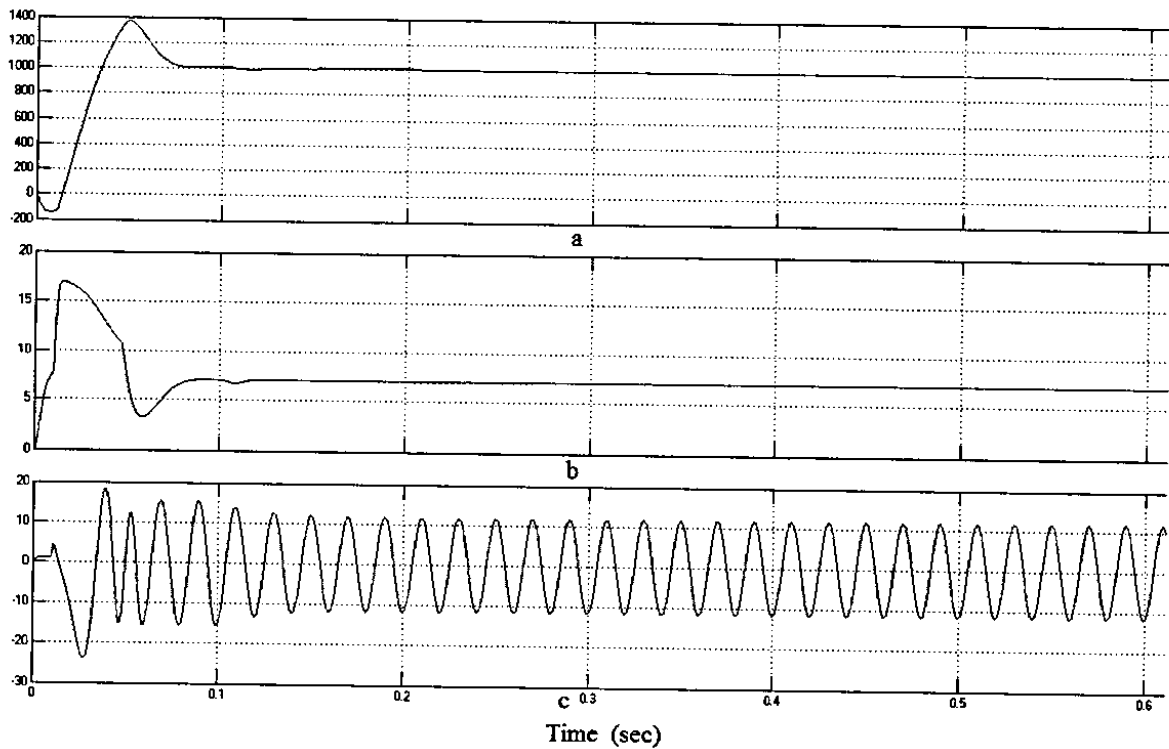
Figure 5.29: (a) speed response (rpm) (b) Developed torque response (N.m) (c) Stator current (A) at 7N.m and 1000 rpm

82
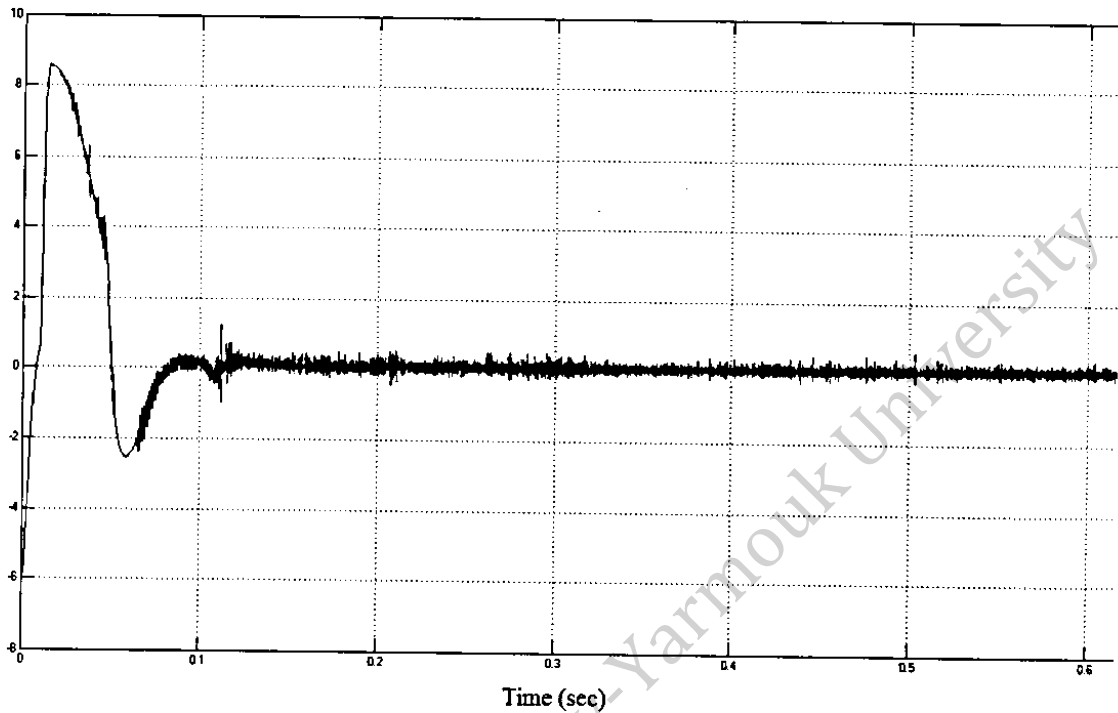
Figure 5.30: Error signal between the actual and estimated rotor speed at 7 N.m and 1000 rpm

Now changing the command speed of the motor to be 500 rpm and changing the motor load torque to be 5 N.m. The speed estimation accuracy should be guaranteed regardless the change in the command speed or the load torque. The simulation results are shown in Figures 5.31 to 5.33. It is clear from the results that the MRAS with FLC is robust in term of changing the command speed or the motor load. Adding the FLC instead of the regular PI controller to the MRAS guarantees the convergence of the estimated speed and reduces the error between the actual and the command rotor speed under different operating conditions.

83

Stator voltage (V) ■

Stator Current (A)

Time (sec)
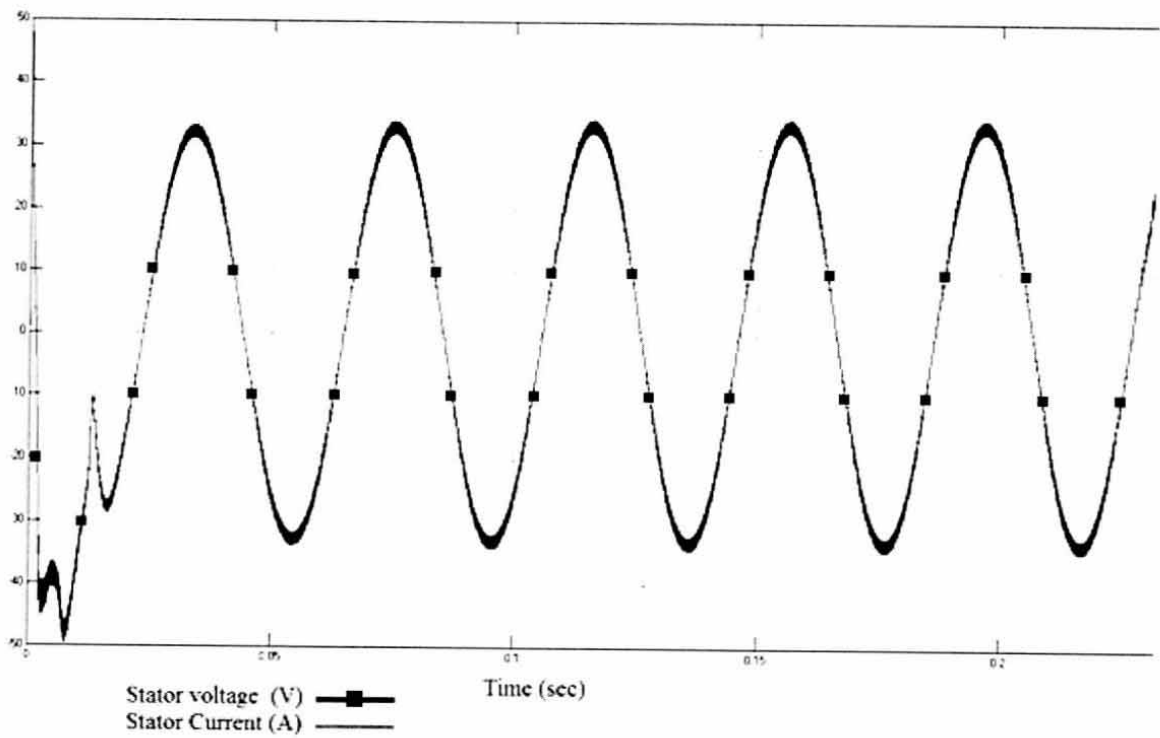
Figure 5.31: Instantaneous stator current and Voltage at 5 N.m and 500 rpm

a

b

c

Time (sec)
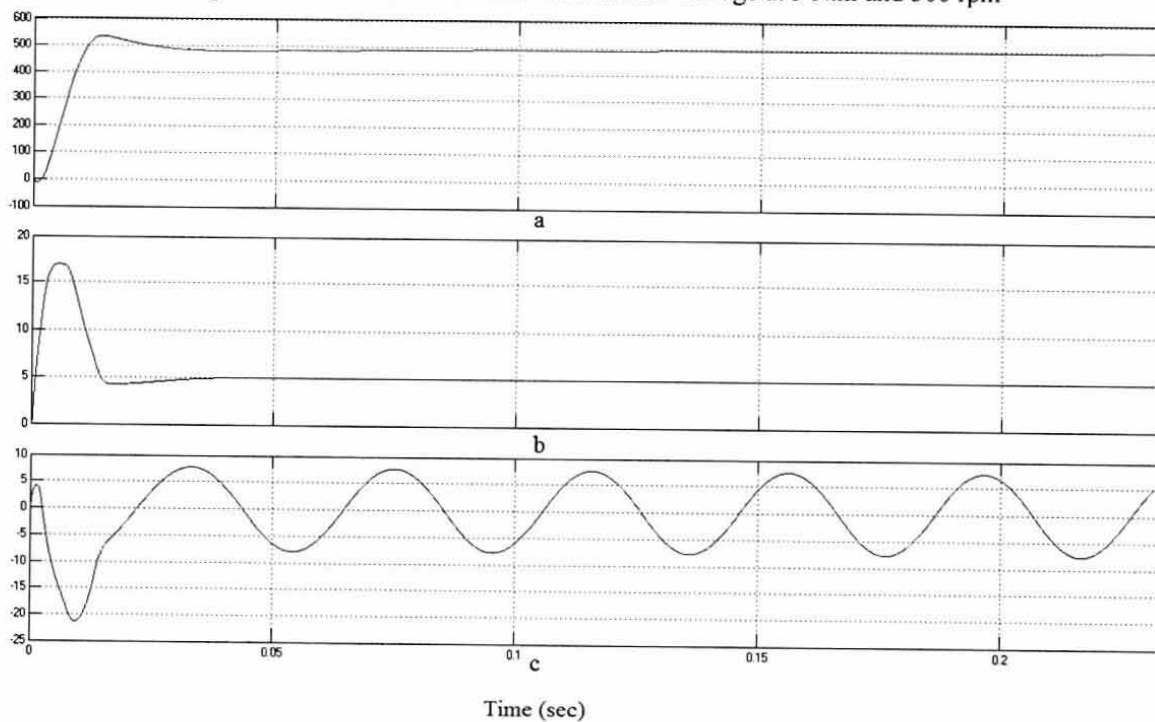
Figure 5.32: (a) speed response (rpm) (b) Developed torque response (N.m) (c) Stator current (A) at 5N.m and 500 rpm

84
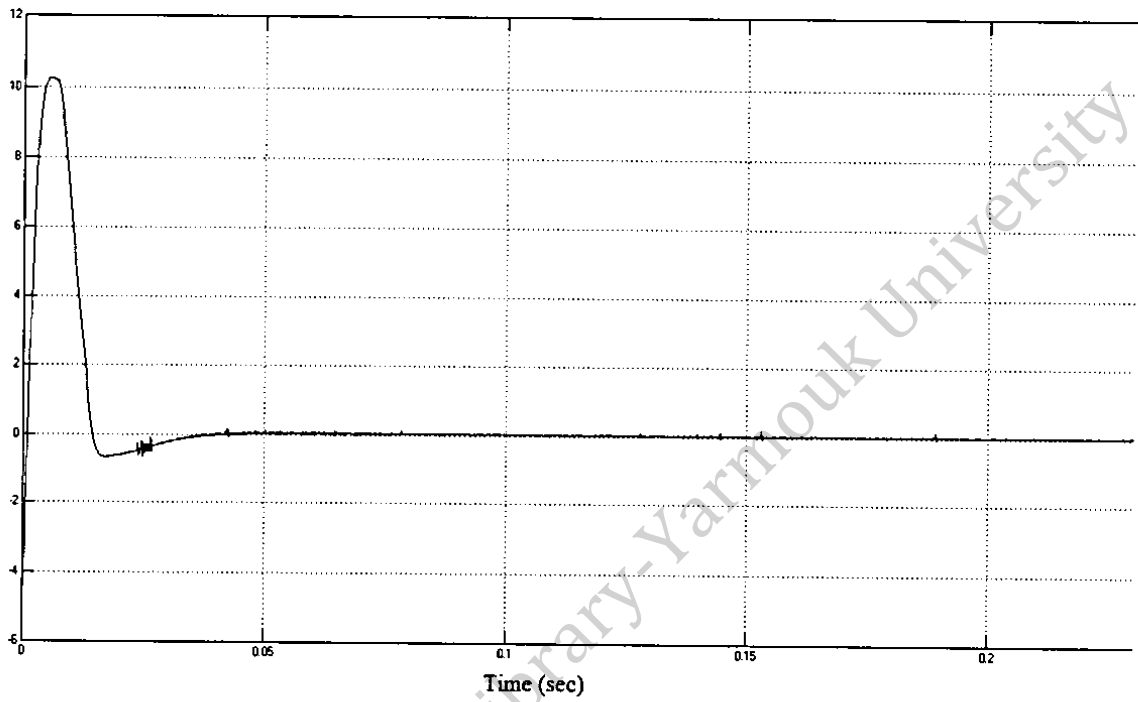
Figure 5.33: Error signal between the actual and estimated rotor speed at 5 N.m and 500 rpm

Chapter 6 CONCLUSION AND FUTURE WORK

6.1 Conclusion

In this thesis; a speed sensorless and unity power factor control of PMSM of surface type has been studied and developed. The new unity power factor control technique in this thesis is simple and requires only a current sensor to measure the q-axis stator current without the need of voltage sensors. This reduced the complexity of the drive system and reduced its cost. The advantage of reducing the VA rating of the inverter and extending the constant torque region of the motor has been showed.

The MRAS –based on the motor's stator current model- for estimating the rotor speed and position has been employed. The simulation results showed that this method is not optimal in terms of the convergence and accuracy of the motor speed response. A SM MRAS has been developed to ensure the stability and convergence of the rotor speed. On the other hand; it requires readapting the sliding mode coefficient when the operating conditions are changed in order reduce the error between the actual and estimated rotor speed. Replacing the PI controller of the MRAS with a FLC was modeled and tested. This method overcomes the problem appeared in the SM MRAS and the accuracy of the estimated speed was guaranteed regardless of any changes made on the motor load torque or the reference speed. However, the modeled FLC is simple and needs only one input membership function to estimate the rotor speed accurately.

6.2 Future Work

Future research work may be of interest concentrating on the following points:

1. Develop a wide speed operation of PMSM to work under constant power region.

2. Explore the possibility of extending the new UPFC for IPMSM.

3. Develop a fuzzy logic control for speed control purpose.

4. To conduct further studies about the impact of harmonics on the UPC.

REFERENCES

[1] Bimal K. Bose, "Modern Power Electronics and AC Drives," Prentice Hall; 1 edition, 2001.

[2] Peter F. Ryff, David Platnick, Joseph A. Karnas, "Electrical machines and Transformers, Principles and Applications", Prentice Hall; First Edition 1987.

[3] "Power Factor Correction (PFC) Handbook". Available: www.onsemi.com.

[4] J. whitaker, "AC power systems handbook", vol. I. 2006.

[5] Moussa, M.F.; Helal, A.; Gaber, Y.; Youssef, H.A.; , "Unity Power Factor control of permanent magnet motor drive system," Power System Conference, 2008. MEPCON 2008. 12th International Middle-East , vol., no., pp.360-367, 12-15 March 2008.

[6] Szabo, C.; Imecs, M.; Incze, I.I.; "Vector control of the synchronous motor operating at unity power factor," Optimization of Electrical and Electronic Equipment, 2008. OPTIM 2008. 11th International Conference on , vol., no., pp.15-20, 22-24 May 2008.

[7] Fang Wu; Shan-ming Wan; Sheng-hua Huang; , "Unity power factor control for PMSM position sensorless drive," Electrical Machines and Systems, 2008. ICEMS 2008. International Conference on , vol., no., pp.1618-1620, 17-20 Oct. 2008.

[8] Zhao Xiaotan; Li Chongjian; Li Yaohua; Wang Chengsheng; , "Analysis of a large power PMSM using different control methods," Electrical Machines and Systems, 2005. ICEMS 2005. Proceedings of the Eighth International Conference on , vol.1, no., pp. 416- 421 Vol. 1, 27-29 Sept. 2005.

[9] Meyer, Michael; Bocker, Joachim; , "Optimum Control for Interior Permanent Magnet Synchronous Motors (IPMSM) in Constant Torque and Flux Weakening Range," *Power Electronics and Motion Control Conference, 2006. EPE-PEMC 2006. 12th International,* vol., no., pp.282-286, Aug. 30 2006-Sept. 1 2006..

[10] Zhu Lei; Xue Shan; Wen Xuhui; Li Yaohua; Kong Liang; , "A new deep field-weakening strategy of IPM machines based on single current regulator and voltage angle control," *Energy Conversion Congress and Exposition (ECCE), 2010 IEEE,* vol., no., pp.1144-1149, 12-16 Sept. 2010.

[11] Yuan Zhang; Longya Xu; Guven, M.K.; Song Chi; Illindala, M.S.; , "Experimental verification of deep flux-weakening operation of a 50 kW IPM machine by using single current regulator," *Energy Conversion Congress and Exposition, 2009. ECCE 2009. IEEE ,* vol., no., pp.3647-3652, 20-24 Sept. 2009.

[12] Consoli, A.; Scarcella, G.; Scelba, G.; Testa, A.; , "Steady-State and Transient Operation of IPMSMs Under Maximum-Torque-per-Ampere Control," Industry Applications, IEEE Transactions on , vol.46, no.1, pp.121-129, Jan.-feb. 2010.

[13] Consoli, A.; Scarcella, G.; Scelba, G.; Sindoni, S.; Testa, A.; , "Steady-State and Transient Analysis of Maximum Torque per Ampere Control for IPMSMs," Industry Applications Society Annual Meeting, 2008. IAS '08. IEEE , vol., no., pp.1-8, 5-9 Oct. 2008.

[14] Ching-Tsai Pan; Sue, S.-M.; , "A linear maximum torque per ampere control for IPMSM drives over full-speed range," Energy Conversion, IEEE Transactions on , vol.20, no.2, pp. 359- 366, June 2005

[15] Islam Chy, M.M.; Uddin, M.N.; , "Analysis of Flux Control for Wide Speed Range Operation of IPMSM Drive," Power Engineering, 2007 Large Engineering Systems Conference on , vol., no., pp.256-260, 10-12 Oct. 2007.

[16] Jabbar, M.A.; Hoque, M.A.; Rahman, M.A.; , "Sensorless permanent magnet synchronous motor drives," *Electrical and Computer Engineering, 1997. IEEE 1997 Canadian Conference on* , vol.2, no., pp.878-883 vol.2, 25-28 May 1997.

[17] Yousfi, D.; Halelfadl, A.; El Kard, M.; , "Sensorless control of Permanent Magnet Synchronous Motor," *Multimedia Computing and Systems, 2009. ICMCS '09. International Conference on* , vol., no., pp.341-344, 2-4 April 2009.

[18] Genduso, F.; Miceli, R.; Rando, C.; Galluzzo, G.R.; , "Back EMF Sensorless-Control Algorithm for High-Dynamic Performance PMSM," *Industrial Electronics, IEEE Transactions on* , vol.57, no.6, pp.2092-2100, June 2010.

[19] Insong Kang; Xiangyun Zeng; Ying Wu; Dabing Hu; , "Study of position sensorless control of PMSM based on MRAS," *Industrial Technology, 2009. ICIT 2009. IEEE International Conference on* , vol., no., pp.1-4, 10-13 Feb. 2009.

[20] Foo, G.H.B.; Rahman, M.F.; , "Direct Torque Control of an IPM-Synchronous Motor Drive at Very Low Speed Using a Sliding-Mode Stator Flux Observer," *Power Electronics, IEEE Transactions on* , vol.25, no.4, pp.933-942, April 2010.

[21] Foo, G.; Rahman, M.F.; , "Sensorless Sliding-Mode MTPA Control of an IPM Synchronous Motor Drive Using a Sliding-Mode Observer and HF Signal Injection," *Industrial Electronics, IEEE Transactions on* , vol.57, no.4, pp.1270-1278, April 2010.

[22] Ying-Shieh Kung; Chung-Chun Huang; Liang-Chiao Huang; , "FPGA-realization of a sensorless speed control IC for IPMSM drive," *IECON 2010 - 36th Annual Conference on IEEE Industrial Electronics Society* , vol., no., pp.1721-1725, 7-10 Nov. 2010.

[23] Foo, G.; Rahman, M.F.; , "Wide-speed direct torque and flux controlled interior permanent-magnet synchronous motor drive using a combined adaptive sliding-mode observer and high-frequency signal injection," *Advanced Electromechanical Motion Systems & Electric Drives Joint Symposium, 2009. ELECTROMOTION 2009. 8th International Symposium on* , vol., no., pp.1-7, 1-3 July 2009.

[24] Young Jo Kim; Hyoung Seok Kang; Young Seok Kim; , "A sensorless speed control of an IPMSM using the observers with the adaptive structure," *Electrical Machines and Systems, 2008. ICEMS 2008. International Conference on* , vol., no., pp.3079-3084, 17-20 Oct. 2008.

[25] Song Chi; Longya Xu; , "Position Sensorless Control of PMSM Based on a Novel Sliding Mode Observer over Wide Speed Range," *Power Electronics and Motion Control Conference, 2006. IPEMC 2006. CES/IEEE 5th International* , vol.3, no., pp.1-7, 14-16 Aug. 2006.

[26] Song Chi; Zheng Zhang; Longya Xu; , "Sliding-Mode Sensorless Control of Direct-Drive PM Synchronous Motors for Washing Machine Applications," Industry Applications, IEEE Transactions on , vol.45, no.2, pp.582-590, March-April 2009.

[27] Li Yongdong; Zhu Hao; , "Sensorless control of permanent magnet synchronous motor — a survey," Vehicle Power and Propulsion Conference, 2008. VPPC '08. IEEE , vol., no., pp.1-8, 3-5 Sept. 2008.

[28] Hakiki, K.; Meroufel, A.; Cocquempot, V.; Chenafa, M.; , "A new adaptive fuzzy vector control for permanent magnet synchronous motor drive," *Control & Automation (MED), 2010 18th Mediterranean Conference on* , vol., no., pp.922-927, 23-25 June 2010

[29] Patil, N.J.; Chile, R.H.; Waghmare, L.M.; , "Hybrid Model Reference Adaptive Fuzzy Controller," *Emerging Trends in Engineering and Technology (ICETET), 2009 2nd International Conference on* , vol., no., pp.698-703, 16-18 Dec. 2009

[30] Nour, M.; Aris, I.; Mariun, N.; Mahmoud, S.; , "Hybrid Model Reference Adaptive Speed Control for Vector Controlled Permanent Magnet Synchronous Motor Drive," *Power Electronics and Drives Systems, 2005. PEDS 2005. International Conference on* , vol.1, no., pp.618-623, 0-0 0.

[31] Hui-ying Dong; Wen-guang Li; Yu Zhao; Kai Lin; "Design and simulation a fuzzy-adaptive PI controller based on MRAS," *Natural Computation (ICNC), 2010 Sixth International Conference on* , vol.5, no., pp.2321-2324, 10-12 Aug. 2010.

[32] Yingpei Liu; Jianru Wan; Guangye Li; Chenhu Yuan; Hong Shen; , "MRAS speed identification for PMSM based on fuzzy PI control," *Industrial Electronics and Applications, 2009. ICIEA 2009. 4th IEEE Conference on* , vol., no., pp.1995-1998, 25-27 May 2009.

[33] Gadoue, S.M.; Giaouris, D.; Finch, J.W.; , "MRAS Sensorless Vector Control of an Induction Motor Using New Sliding-Mode and Fuzzy-Logic Adaptation Mechanisms," *Energy Conversion, IEEE Transactions on* , vol.25, no.2, pp.394-402, June 2010.

[34] Gadoue, S.M.; Giaouris, D.; Finch, J.W.; , "A new fuzzy logic based adaptation mechanism for MRAS sensorless vector control induction motor drives," *Power Electronics, Machines and Drives, 2008. PEMD 2008. 4th IET Conference on* , vol., no., pp.179-183, 2-4 April 2008.

[35] Adam, A.A; Gulez, K.; "Torque Control of PMSM and Associated Harmonic Ripples"; ISBN 978-953-307-428-3, February 2011.

APPENDIX A

The m-file which calculates the performance of SPMSM under UPFC and

MTPA is listed below:

```
clc;
%*************************
% SPMSM PARAMETERS
%*************************
R=1.4;        % Stator Resistance (ohm)
L=0.0066;     % Stator inductance (H)
Ym=0.1546;    % PM Flux Linkage (web)
P=6;          % Number of Poles
%*************************
% Torque & Speed Reference
%*************************
Te=7;
nm=1000;
ne=(P/2)*nm;
%*************************
%   UPFC steady state char.
%*************************
we=2*pi*ne/60
wm=(2/P)*we
Iq=Te*(2/3)*(2/P)*(1/Ym)                    %Iq stator current
Id_ref=(-Ym+sqrt(Ym^2-4*L^2*Iq^2))/(2*L)   %reference Id current for UPF
Vq=0.5*(we*Ym+2*Iq*R+sqrt((we*Ym+2*Iq*R)^2-
4*(we^2*L^2*Iq^2+we*Ym*Iq*R+Iq^2*R^2)))
Vd=(-we*Iq*Vq*L)/(Vq-Iq*R)
Vs_UPF=sqrt(Vq^2+Vd^2)                      %the amplitude of the stator voltage
Is_UPF=sqrt(Iq^2+Id_ref^2)                  %the amplitude of the stator current
%*************************
%Id=Zero for MTPA
%*************************
Vd_0Id=-we*L*Iq
Vq_0Id=R*Iq+we*Ym
Vs2=sqrt(Vd_0Id^2+Vq_0Id^2)                 %the amplitude of the stator voltage
Is2=Iq                                      %the amplitude of the stator current
%*************************
%   Performance Curves
%*************************
w(1,1)=0;
Ne(1,1)=0;
Nm(1,1)=0;
%*************************
% UPFC
%*************************
for i=1:120
    iq(1,i)=Te*(2/3)*(2/P)*(1/Ym);
    id(1,i)=(-Ym+sqrt(Ym^2-4*L^2*iq(1,i)^2))/(2*L);
```

94

```matlab
    vq(1,i)=0.5*(w(1,i)*Ym+2*iq(1,i)*R+sqrt((w(1,i)*Ym+2*iq(1,i)*R)^2-
       4*(w(1,i)^2*L^2*iq(1,i)^2+w(1,i)*Ym*iq(1,i)*R+iq(1,i)^2*R^2)));
    vd(1,i)=(-w(1,i)*iq(1,i)*vq(1,i)*L)/(vq(1,i)-iq(1,i)*R);
    vs(1,i)=sqrt(vq(1,i)^2+vd(1,i)^2);
    is(1,i)=sqrt(iq(1,i)^2+id(1,i)^2);
    if i~=120
        w(1,i+1)=w(1,i)+5;
        Ne(1,i+1)=w(1,i+1)*30/pi;
        Nm(1,i+1)=(2/P)* Ne(1,i+1);
    end
end

%************************
% MTPA
%************************
for i=1:120
    iq2(1,i)=Te*(2/3)*(2/P)*(1/Ym);
    id2(1,i)=0;
    vq2(1,i)=R*iq2(1,i)+w(1,i)*Ym;
    vd2(1,i)=-w(1,i)*iq2(1,i)*L;
    vs2(1,i)=sqrt(vq2(1,i)^2+vd2(1,i)^2);
    is2(1,i)=sqrt(iq2(1,i)^2+id2(1,i)^2);
    if i~=120
        w(1,i+1)=w(1,i)+5;
        Ne(1,i+1)=w(1,i+1)*30/pi;
        Nm(1,i+1)=(2/P)* Ne(1,i+1);
    end
end

%**************************
% Torque vs Is at constant speed command
%**************************
T(1,1)=0;
for i=1:70
    iq3(1,i)=T(1,i)*(2/3)*(2/P)*(1/Ym);
    id3(1,i)=(-Ym+sqrt(Ym^2-4*L^2*iq3(1,i)^2))/(2*L);
    vq3(1,i)=0.5*(we*Ym+2*iq3(1,i)*R+sqrt((we*Ym+2*iq3(1,i)*R)^2-
       4*(we^2*L^2*iq3(1,i)^2+we*Ym*iq3(1,i)*R+iq3(1,i)^2*R^2)));
    vd3(1,i)=(-we*iq3(1,i)*vq3(1,i)*L)/(vq3(1,i)-iq3(1,i)*R);
    vs3(1,i)=sqrt(vq3(1,i)^2+vd3(1,i)^2);
    is3(1,i)=sqrt(iq3(1,i)^2+id3(1,i)^2);
    is33(1,i)=iq3(1,i);
    if i~=70
        T(1,i+1)=T(1,i)+0.1;
    end
end
%******************************************
figure (1);
clf
plot(Nm,vs,'b')
hold on
plot (Nm,vs2,'r')
xlabel('n_m [rpm]');
ylabel('Phase Voltages (peak value) [V]');
set(gca,'YLim',[0 100]); %Vsmax
box on;
legend('UPFC','MTPAC',4);
```

95

```
grid on;
%*********************************************
figure (2);
clf
plot(Nm,is)
hold on
plot (Nm,is2,'r')
xlabel('n_m [rpm]');
ylabel('Phase Currents (peak value) [A]');
box on;
legend('UPFC','MTPAC',4);
grid on;
%*********************************************
figure (3);
clf
plot(T,is3)
xlabel('Torque [Nm]');
ylabel('Phase Currents (peak) [A]');
box on;
grid on;
%*********************************************
figure (4);
clf
plot(T,is3)
hold on
plot (T,is33,'r')
xlabel('Torque [Nm]');
ylabel('Phase Currents (peak) [A]');
box on;
legend('UPFC','MTPAC',4);
grid on;
```

96

الملخص

شحاده، حكم سليمان. التحكم بالسرعة بواسطة معامل القدرة الأحادي عديم المجسات للمحركات التوافقية ذات المغناطيسة الدائمة. رسالة ماجستير في قسم هندسة الحاسوب، كلية الحجاوي للهندسة التكنولوجية، جامعة اليرموك. 2011

(المشرف الرئيس: د. محمد الزعبي، المشرف المشارك: د. سامي الحمدان)

هناك العديد من أساليب التحكم في أنظمة القيادة للمحركات التوافقية ذات المغناطيسية الدائمة. في هذا العمل، تم تطوير نظام جديد للتحكم بمعامل القدرة الأحادي للمحركات التوافقية ذات المغناطيسية الدائمة ثلاثية الطور مع التحكم بالسرعة عديم المجسات وذلك باستخدام نظام النموذج المرجعي المتكيف المعتمد على تحكم المنطق الضبابي. العمل الحالي يضمن التشغيل بمعامل القدرة الأحادي للمحرك بحيث أن الجهد والتيار للمحرك يكونان متماثلا الطور ولا يوجد بينهما فرق بزاوية الطور. لقد تم تحقيق التحكم بسرعة المحرك وذلك عن طريق استخدام نظام النموذج المرجعي المتكيف والذي يعمل على تقدير سرعة المحرك دون استخدام مجسات ميكانيكية لقياس السرعة. تم استخدام نظام المنطق الضبابي بالتزامن مع نظام النموذج المرجعي المتكيف وذلك لتقليل الخطأ في حالة الاستقرار ما بين سرعة المحرك الحقيقية والسرعة المقدرة تحت أحمال و أوامر سرعة مختلفة.

تم نمذجة وحدة التحكم و محاكاتها و ذلك باستخدام برنامج المحاكاه ماتلاب-سيمولينك. وقد تم إجراء مقارنة بين نظام تحكم عزم الدوران الأقصى لكل أمبير ونظام تحكم معامل القدرة الأحادي. تم إجراء مقارنة أخرى بين نظام النموذج المرجعي المتكيف المعتمد على تحكم المنطق الضبابي ونظام النموذج المرجعي المتكيف الذي يستخدم أسلوب تحكم النمط المنزلق حيث أكدت النتائج متانة النظام المنمذج للتحكم بالسرعة عديم المجسات تحت ظروف تشغيل مختلفة للمحرك. كما أجريت العديد من الدراسات لحالات مختلفة وتم إظهار نتائج المحاكاه لها حيث أثبتت صحة ودقة نهج نظام التحكم المستخدم.

الكلمات المفتاحية: المحركات التوافقية ذات المغناطيسية الدائمة، التحكم بمعامل القدرة الأحادي، التحكم بالسرعة عديم المجسات، نظام النموذج المرجعي المتكيف، تحكم النمط المنزلق، تحكم المنطق الضبابي.